

Turning Organic Reducing Agents Catalytic

by

Zachary Rees

Bachelor of Science, Honors in Medicinal Chemistry, University of New Brunswick,
2020

A Thesis Submitted in Partial Fulfillment
of the Requirements for the Degree of

Master of Science

in the Graduate Academic Unit of Chemistry

Supervisor: C. Adam Dyker, PhD, Chemistry

Examining Board: Andreas Decken, PhD, Chemistry
Chris McFarlane, PhD, Earth Sciences

This thesis is accepted by the
Dean of Graduate Studies

THE UNIVERSITY OF NEW BRUNSWICK

December 2021

© Zachary Lucas Rees, 2021

Abstract

Bispyridinylidenes (BPYs) are a class of organic reducing agents (ORAs), which can be used to perform homogenous reductions under mild conditions that many classical reducing agents such as alkali metals cannot. Generally speaking, the molecular weights for BPYs far exceed those of the substrates, and most reductions employ an excess of BPY. This causes large scale reductions to be difficult, the overall cost of the reductions to be high, and difficulties during purification due to a large mass of BPY byproduct. In order to rectify these problems a two-component catalytic cycle was envisioned that involves sub-stoichiometric amounts of BPY as the active species for substrate reduction, and a sacrificial electron donor (SD) that continually regenerates the BPY from its oxidized form. A Cy₃PN-substituted BPY was chosen for this study based on its strong reduction potential, ease of preparation in both the reduced and oxidized forms, and it features phosphorus for easy monitoring of reactions by ³¹P NMR spectroscopy. This BPY was used to reduce several phosphorous based substrates. Many sacrificial donors were tested however, only sodium appeared to be a viable option for the regeneration of the BPY from its oxidized form. The potential of this new two-component catalytic cycle is demonstrated through the successful reduction of dichlorotricyclohexylphosphorane (Cl₂PCy₃) producing tricyclohexylphosphine (PCy₃) using catalytic amounts (5-20 mol %) of the BPY along with an excess of sodium. Reductions were also attempted using only the sacrificial donor as a control which proved the necessity of the ORA.

Acknowledgements

I would like to thank Dr. C. Adam Dyker for all the help and guidance that he has provided me with throughout my entire program. He was more than supportive both in and out of the lab, and I could not have asked for a better supervisor. I am grateful to have been a member of the Dyker group for the past three years. I would also like to thank the current and previous members of the Dyker group for supporting me in my research and for taking the time to teach me whatever they could, especially when it pertained to lab techniques. My time spent in the group was extremely enjoyable and lots of great memories were made with a great group of people. Furthermore, I would like to thank my advisory committee, Dr. James Tait, and Dr. Andreas Decken, as well as my thesis readers and examiners for their contributions.

Additionally, I would like to thank my friends in the chemistry department who have supported me along the way. Finally, I would also like to extend my deepest gratitude to my family for their continuous love, support, and encouragement.

Table of Contents

Abstract	ii
Acknowledgements	iii
Table of Contents	iv
List of Schemes	v
List of Tables.....	vii
List of Figures	viii
List of Symbols, Nomenclature or Abbreviations.....	xi
Chapter 1: Introduction.....	1
Chapter 2: Catalytic Cycle Development and Substrate Testing	13
2.1: Introduction	13
2.2: Results and Discussion	15
2.3: Conclusion and Future Work	48
Chapter 3: Experimental	53
3.1: General Considerations.....	53
3.2: General Synthetic Procedures	54
3.3: Sodium activation.....	59
3.4: Regeneration Stage General Procedures	60
3.5: Reduction Stage General Procedures.....	62
3.6: Control Stage General Procedures.....	65
3.7: Catalytic Cycle General Procedures	69
Bibliography.....	73
Appendix A.....	78
Curriculum Vitae	

List of Schemes

Scheme 1.1: Reductive cleavage of alkyl triflate by ORA vs. metal reductant	2
Scheme 1.2: Carbocation stabilization of sulphur vs. nitrogen.	3
Scheme 1.3: Oxidation of a BPY compound.....	4
Scheme 1.4: Stabilization of oxidized BPY through resonance.	5
Scheme 1.5: Reversibility of BPY compounds	8
Scheme 1.6: Catalytic process using ORA 1.14 in a catalytic amount to reduce substrate X-R ₁ , forming product H-R ₂	9
Scheme 1.7: Protonation of anion intermediate from an oxidized BPY species.	10
Scheme 1.8: Typical reductions using BPY compounds.	11
Scheme 1.9: Proposed catalytic cycle.	12
Scheme 2.1: Proposed catalytic cycle and control stage.....	14
Scheme 2.2: Formation of 2.3 following Hanson's synthetic pathway.	16
Scheme 2.3: Improved synthetic pathway for the formation of 2.3	17
Scheme 2.4: Synthetic pathway for the formation of BPY 1.12 ²⁺ 2I ⁻	19
Scheme 2.5: Catalytic cycle with chosen BPY 1.12	20
Scheme 2.6: Catalytic cycle with chosen BPY (1.12) and SD (Na).	24
Scheme 2.7: Reduction of halogenated phosphoranes using BPY 2.5	25
Scheme 2.8: Reduction of dichlorotricyclohexylphosphorane 2.6 to phosphine 2.7 through the use of 1.12 (formed <i>in situ</i>).	26
Scheme 2.9: Control test for the reduction of 2.6 with sodium.	28
Scheme 2.10: Full catalytic cycle showing all chosen species	29

Scheme 2.11: A: equilibrium between pentavalent and tetravalent geometry in phosphoranes. B: Metathesis of 2.6' with 1.12²⁺2I⁻	31
Scheme 2.12: Metathesis reaction between 2.6' and varying equivalents of 1.12²⁺2I⁻	32
Scheme 2.13: Iodine addition and its effects on each stage of the catalytic cycle.	35
Scheme 2.14: Catalytic cycle for the reduction of 2.6	38
Scheme 2.15: Proposed catalytic cycle for the reduction of 2.8	41
Scheme 2.16: Reduction of 2.8 through the use of 1.12 formed <i>in situ</i>	42
Scheme 2.17: Reduction of 2.8 through the use of Na.	43
Scheme 2.18: Synthesis of dichlorotriphenylphosphorane (2.13).	44
Scheme 2.19: Reduction of 2.13 via 1.12 (generated <i>in situ</i>).	45
Scheme 2.20: Reduction of 2.13 via activated Na.	46
Scheme 2.21: General reduction of a carbene precursor and silane derivative through the use of 0.05 eq 1.12 , 40 eq Na*, THF.	49
Scheme 2.22: Proposed biphasic catalytic cycle.	51
Scheme 2.23: Proposed electrochemical catalytic cycle.	52

List of Tables

Table 1.1: Change in reduction potentials by varying substituents on BPY 1.9	5
Table 1.2: BPY compounds with iminophosphorano substituents.	7
Table 2.1: Sacrificial donors tested for use in the regeneration stage.	21

List of Figures

Figure 1.1: Classical ORAs and their corresponding redox potentials vs. SCE	1
Figure 1.2: Tetra-substituted BPY vs. di-substituted BPY.....	7
Figure 2.1: ^{31}P NMR spectrum of compound 2.3 in CDCl_3	17
Figure 2.2: ^1H NMR spectrum of compound 2.3 in CDCl_3	18
Figure 2.3: ^{31}P spectrum of compound 1.12$^{2+}2\text{I}^-$ in CDCl_3	19
Figure 2.4: ^1H NMR spectrum of compound 1.12$^{2+}2\text{I}^-$ in CDCl_3	20
Figure 2.5: Stacked ^{31}P NMR spectra, monitoring the reduction of 1.12$^{2+}2\text{I}^-$ via Na in THF over 15 hours.....	23
Figure 2.6: Z and E isomers of 1.12	24
Figure 2.7: ^{31}P NMR spectrum of the reaction mixture of the reduction of 2.6 in THF via BPY 1.12 (generated <i>in situ</i>) after 10 minutes.....	27
Figure 2.8: Stacked ^{31}P NMR spectra, monitoring the reduction of 2.6 via Na in THF over 18h.....	28
Figure 2.9: Stacked ^{31}P NMR spectra monitoring the reduction of 2.6 with 25 eq of 1.12$^{2+}$ and 40 eq of Na in THF.....	30
Figure 2.10: Metathesis reaction between 2.6 and 0.5eq of 1.12$^{2+}2\text{I}^-$	33
Figure 2.11: Stacked ^{31}P NMR spectra, monitoring the reduction of 1.12$^{2+}2\text{I}^-$ via Na^* in THF.....	36
Figure 2.12: Stacked ^{31}P NMR spectra, monitoring the reduction of 2.6 via Na^* in THF over 24.5 hours.....	37
Figure 2.13: Stacked ^{31}P NMR spectra, monitoring the reduction of 2.6 via the optimized catalytic cycle with 25% catalytic loading.....	38

Figure 2.14: Stacked ^{31}P NMR spectra, monitoring the reduction of 2.6 via the optimized catalytic cycle with 12.5% catalyst loading.	39
Figure 2.15: Stacked ^{31}P NMR spectra, monitoring the reduction of 2.6 via the optimized catalytic cycle with 5% catalyst loading.	40
Figure 2.16: ^{31}P NMR spectrum of pure substrate 2.8 (bottom spectrum). ^{31}P NMR spectrum of the reaction mixture 10 minutes after the addition of 2.8 to BPY 1.12 (formed <i>in situ</i> , (top spectrum)).	42
Figure 2.17: ^{31}P NMR spectrum of the reaction mixture 10 minutes after the addition of 2.8 to Na^* in THF.	44
Figure 2.18: ^{31}P NMR spectrum of pure substrate 2.13 in THF (bottom spectrum). ^{31}P NMR spectrum of the reaction mixture 10 minutes after the addition of 2.13 to BPY 1.12 (formed <i>in situ</i> , (top spectrum)).	45
Figure 2.19: Stacked ^{31}P NMR spectra, monitoring the reduction of 2.13 via Na^* over 1.5h.	47
Figure A1: ^1H NMR spectra of 1-methyl-4-aminopyridine in D_2O	77
Figure A2: ^{31}P NMR spectra of BPY 1.12 (<i>in situ</i>) formation from 2.3 in toluene.	78
Figure A3: Stacked ^{31}P NMR spectra, monitoring the reduction of 1.12 $^{2+}2\text{I}^-$ with Li in THF over 23.5 hours.	78
Figure A4: Stacked ^{31}P NMR spectra, monitoring the reduction of 1.12 $^{2+}2\text{I}^-$ with Mg in THF over 2.5 days.	79
Figure A5: Stacked ^{31}P NMR spectra, monitoring the reduction of 1.12 $^{2+}$ with K in THF over 2h.	79
Figure A6: ^{31}P NMR of dichlorotriphenylphosphorane (2.13) in acetonitrile.	80

Figure A7: ^{31}P NMR spectrum of **2.6** and 1eq. of iodine.....80

List of Symbols, Nomenclature or Abbreviations

ORA.....	Organic reducing agent
OED.....	Organic electron donor
BPY.....	Bispyridinylidene
DMAP.....	4-dimethylaminopyridine
R.....	Substituent
SCE.....	Saturated calomel electrode
BPY ²⁺	Oxidized BPY
<i>p</i> -tol.....	Tri(<i>p</i> -tolyl)phosphine
<i>p</i> -C ₆ H ₄ Cl.....	Tri(4-chlorophenyl)phosphine
Ph.....	Phenyl
Cy.....	Cyclohexyl
CV.....	Cyclic voltammetry
σ_p^+	Hammett-type substituent constant
DMF.....	Dimethylformamide
R ²	Linear correlation squared
TEP.....	Tolman electronic parameters
PRC.....	Polarity reversal catalyst
SD.....	Sacrificial donor
THF.....	Tetrahydrofuran
OPCy ₃	Tricyclohexylphosphine oxide
Cl ₂ PCy ₃	Dichlorotricyclohexylphosphorane

ClPPh ₂	Chlorodiphenylphosphine
Cl ₂ PPh ₃	Dichlorotriphenylphosphorane
X.....	Halogen functional group
³¹ P NMR.....	Phosphorous nuclear magnetic resonance
¹ H NMR.....	Proton nuclear magnetic resonance

Chapter 1: Introduction

Organic reducing agents (ORAs such as representative examples (**1.1-1.5**)) are a class of organic electron donors (OEDs)¹ capable of transferring electrons at relatively low potentials. These neutral organic compounds have been proven capable of successfully reducing substrates such as sulfones,² arenesulfonamides,³ halogenated arenes,⁴ halogenated phosphines,⁵ triflamdes,⁶ acyloin derivatives,⁷ and Weinreb amides.⁸ Before the development of ORAs such reductions would only have been expected from the use of strong inorganic reducing agents such as alkali metals.⁹ In addition, ORAs were found to be capable of reducing unactivated benzenes, creating free radical anions, and are able to reductively cleave aryl-halides.^{3,4,10}

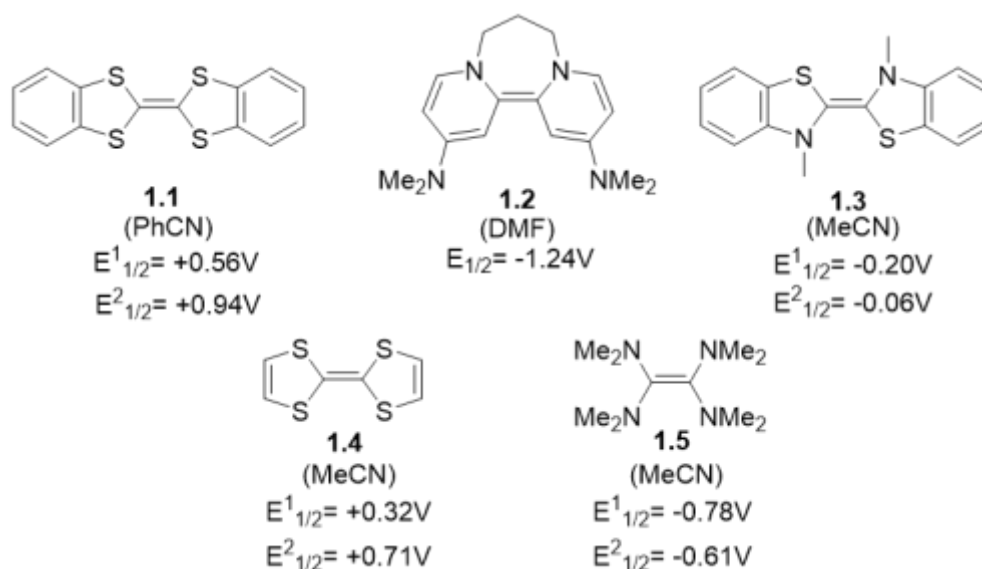
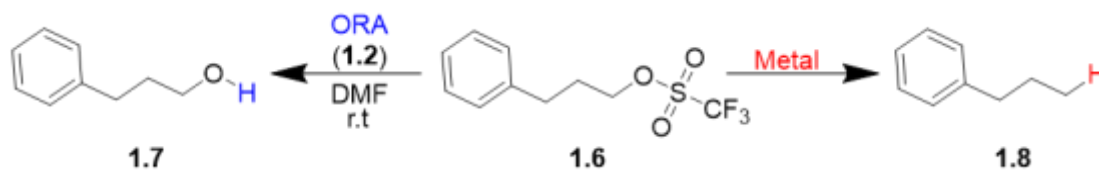


Figure 1.1: Classical ORAs and their corresponding redox potentials vs. SCE.^{3,9}

Reductions can be performed using ORAs in their ground state configurations, under relatively mild conditions^{10,11} because ORAs are soluble in many aprotic solvents, forming homogeneous mixtures. This is unlike many traditional reductions that require

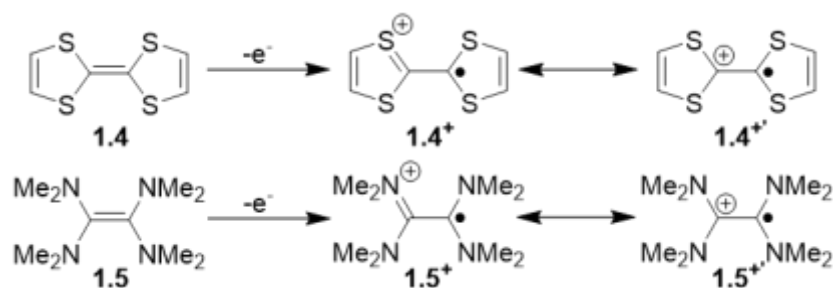
highly reactive metals such as lithium, sodium or potassium to facilitate the reaction.¹² Reductions performed by alkali metals are often slow surface area reactions (heterogenous) unless performed in certain amine solvents such as ammonia (liquid) which allows for the generation of solvated electrons.¹² Alkali metals that are used for reductions are generally highly reactive and undergo exothermic reactions with water,¹³ making them difficult to use. Many ORAs display better selectivity at lower temperatures (room temperature) when compared to alkali metals which generally require higher temperatures¹⁴ (often to melt the metal and increase its active surface area) to successfully perform reductions at efficient rates.¹⁰ ORAs are also tolerant to various functional groups such as alcohols, carboxyl, nitro, carbonyl, ester, and cyano groups.¹⁵ It has also been found that when using an ORA and a metal to perform the same reduction, different products can be obtained (**Scheme 1.1**).¹⁶



Scheme 1.1: Reductive cleavage of alkyl triflate by ORA vs. metal reductant.¹⁷

Scheme 1.1 demonstrates that when using an ORA to deprotect an alkyl triflate, cleavage occurs between the O-S bond. Alternatively, when using potassium to deprotect the alkyl triflate cleavage occurs between the C-O bond. **Scheme 1.1** is a good example of the functionality of both ORAs and metals as reducing agents. In this case, the ORA is able to act as a mild reducing agent as opposed to the metal which is able to cleave the stronger C-O bond. This also illustrates the complementarity of the two types of reagents.

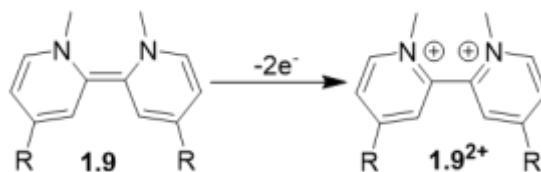
ORAs are typically composed of a π -system and electron rich substituents (involving nitrogen (N) or sulphur (S) bearing lone pairs). Many different ORAs have been developed and cover a wide range redox potentials.⁹ It was found that when nitrogen is the heteroatom (**1.2**) as opposed to sulphur (**1.4**) in the heterocyclic ring it is able to contribute more electron density into the π system of the ORA.⁴ Since it is easier to transfer electrons from electron-rich systems, reducing agents with more electron density are inherently stronger donors (**1.2**, **1.5**).⁴ Additionally, it was found that ORAs containing nitrogen as opposed to sulfur have better resonance stabilization of the resulting oxidized ORA due to more favorable orbital overlap to the adjacent carbocation (2p-2p vs. 3p-2p **Scheme 1.2**). The more electron rich neutral form of the ORA, and the more stabilized oxidized form of the ORA both contribute to more negative reduction potentials (i.e., the neutral compound is a stronger reducing agent).



Scheme 1.2: Carbocation stabilization of sulphur vs. nitrogen.

The most studied series of ORAs to date are bispyridinylidene (BPY) derivatives. The first BPY was developed in 2008 by Murphy et al. (**1.2**), it was derived from 4-dimethylaminopyridine (DMAP). This DMAP derived BPY has a low redox potential, is easily prepared, and is able to transfer two electrons, making it a versatile and effective reducing agent.^{4,9} With the development of this strongly reducing ORA it was found that

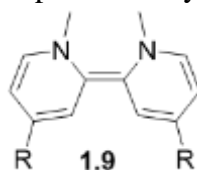
there are several different factors that affect the electrochemical properties and overall redox potential. Once a BPY reduces a substrate it becomes oxidized, this creates aromaticity within the main scaffold of the BPY, further stabilizing the compound and acting as a driving force of the reduction. (**Scheme 1.3**).^{6,18,19}



Scheme 1.3: Oxidation of a BPY compound.

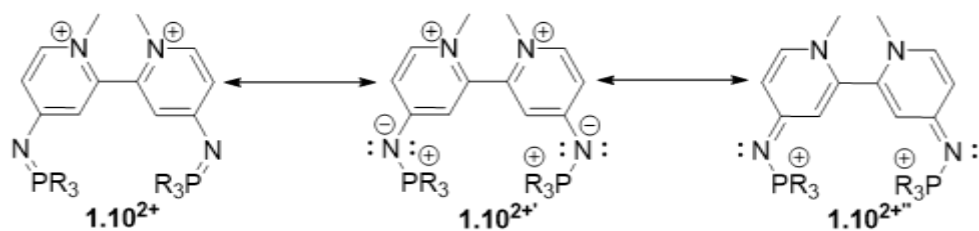
In addition to the work done by Murphy et al., Clennan and his colleagues were able to develop a small library of compounds demonstrating that many BPYs have much lower reduction potentials than most classical ORAs such as tetrakis(dimethylamino)ethylene (**1.5**)²⁰ and tetrathiafulvalene (**1.4**).^{19,21} This is because BPY derivatives have highly tunable scaffolding and their overall electrochemical properties can be easily modified by changing their exocyclic substituents, (**Table 1.1**) leading to lower redox potentials.^{15,19,22}

Table 1.1: Change in reduction potentials by varying substituents on BPY **1.9**.¹⁹



Compound	Substituent (R)	$E_{1/2}$ (V vs. SCE) (CH ₃ CN)
1.9a	-N(Me) ₂	-1.35
1.9b	-OMe	-0.97
1.9c	-H	-0.76
1.9d	-Cl	-0.60
1.9e	-CO ₂ Me	-0.26

With the development of these new BPYs it was found that the nature of the exocyclic substituents on the BPY greatly effects the overall electrochemical properties and redox potential of the compound. This inspired Dyker et al. to use highly donating iminophosphorano groups (R₃P=N-) as the exocyclic substituents in an effort to prepare some of the most donating ORAs to date.¹⁵ By using better electron donating groups as the exocyclic substituents, the stability of the oxidized BPY (BPY²⁺) is increased,¹⁸ leading to more negative redox potentials compared to other derivatives (**Scheme 1.4**).

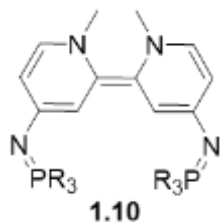


Scheme 1.4: Stabilization of oxidized BPY through resonance.

The donating strength of the R group attached to the phosphine in iminophosphorano substituted BPY derivatives has a large impact on the strength of the reducing agent. When R is more donating it is able to better stabilize the positive charge on the phosphorous atom (1.10^{2+}), this makes the nitrogen atom more negative and a stronger π donor (**Scheme 1.4**). This means that iminophosphorano-substituted BPYs with alkyl R groups are stronger reducing agents than BPYs with aryl R groups [sp^3 hybridized carbon vs. sp^2 hybridized carbon which is slightly withdrawing via the π^* system]. This effect can be seen in the experimental data in **Table 1.2**.^{15,23}

Dyker et al. was able to create a series of some of the strongest BPYs to date and determine the Hammett constants (σ_p^+) of the substituents ($R_3P=N^-$).²³ The Hammett constant σ_p^+ represents a substituent constant designed for cases where the substituent involves a donor atom in direct conjugation with a positively charged reaction center.²³ The linear relation between the overall redox potential of a compound and its σ_p^+ value shows us that BPY compounds containing strong exocyclic electron donating groups (more negative σ_p^+ values) will lead to compounds with stronger redox potentials (**Table 1.2**). It was found that these values correlate to the known Tolman electronic parameter (TEP) values of the corresponding phosphine functional groups (R_3P) and the overall reduction potentials of the BPY compounds. The TEP is a measure of the electron donating/withdrawing ability of a ligand (R_3P here), quantified from the measured CO stretching frequency of the $L-Ni(CO)_3$ complex, where more donating ligands are associated with a lower TEP value.²⁴ By relating σ_p^+ to the corresponding TEP value of R_3P , it is possible to predict the redox potential of a wide range of BPYs featuring $R_3P=N^-$ substituents.²³

Table 1.2: BPY compounds with iminophosphorano substituents.



Compound	Substituent (R)	$E_{1/2}$ (V vs. SCE) (DMF)	σ_p^+ ($R_3P=N-$)	TEP (R_3P) cm^{-1}
1.10a	<i>p</i> -tol	-1.38	-1.92	2066.7
1.10b	-Ph	-1.34	-1.82	2068.9
1.10c	<i>p</i> -C ₆ H ₄ Cl	-1.30	-1.72	2072.8
1.10d	-Cy	-1.51	-2.23	2056.4

Following the studies showing the correlation of strong donating groups to overall redox potential, Dyker and Murphy et al. investigated the change in redox potential between BPY compounds that were tetra-substituted and di-substituted (**Figure 1.2**).²⁵

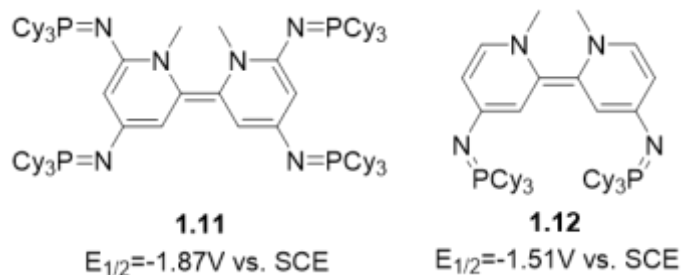
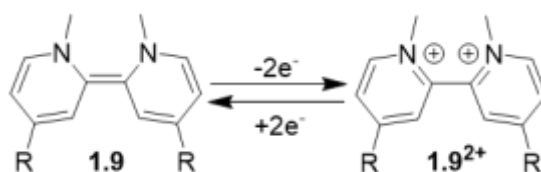


Figure 1.2: Tetra-substituted BPY vs. di-substituted BPY.

It was found that tetra-substituted BPY derivatives will be stronger reducing agents than their corresponding di-substituted BPY with the same substituents. This is because a tetra-substituted BPY contains more electron donating groups than the di-substituted BPY

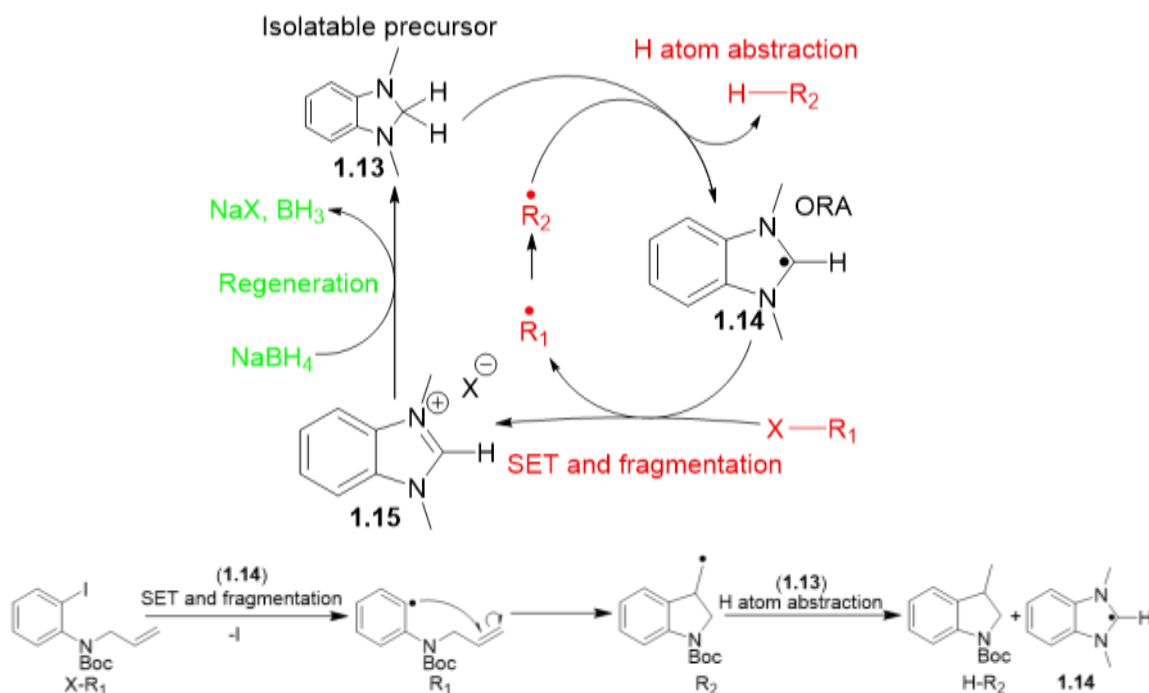
allowing for better stabilization of the oxidized BPY species. The additional electron donating groups also cause the neutral compound to be more electron rich, this means that the highest occupied molecular orbital (HOMO) of the tetra-substituted BPY is higher in energy than its di-substituted counterpart. This held true for all substituents that were used for both di and tetra substituted BPYs.²⁵

Many BPYs and their oxidized counterparts have been isolated separately as stable species. The oxidization of BPY compounds is a reversible process (**Scheme 1.5**).³ This brings forward the possibility to exchange between the two species by successive redox events, opening up the possibility to use these reducing agents in a catalytic manner.



Scheme 1.5: Reversibility of BPY compounds.²⁶

In 2019 Murphy et al. developed a catalytic process using an ORA (**1.14**) as the catalyst. Using this catalytic process, Murphy et al. was able to reduce a series of aryl halides and alkyl halides in moderate to relatively good yields. This the first time that an ORA was used in a catalytic manner to perform reductions at sub-stoichiometric amounts (**Scheme 1.6**).²⁷

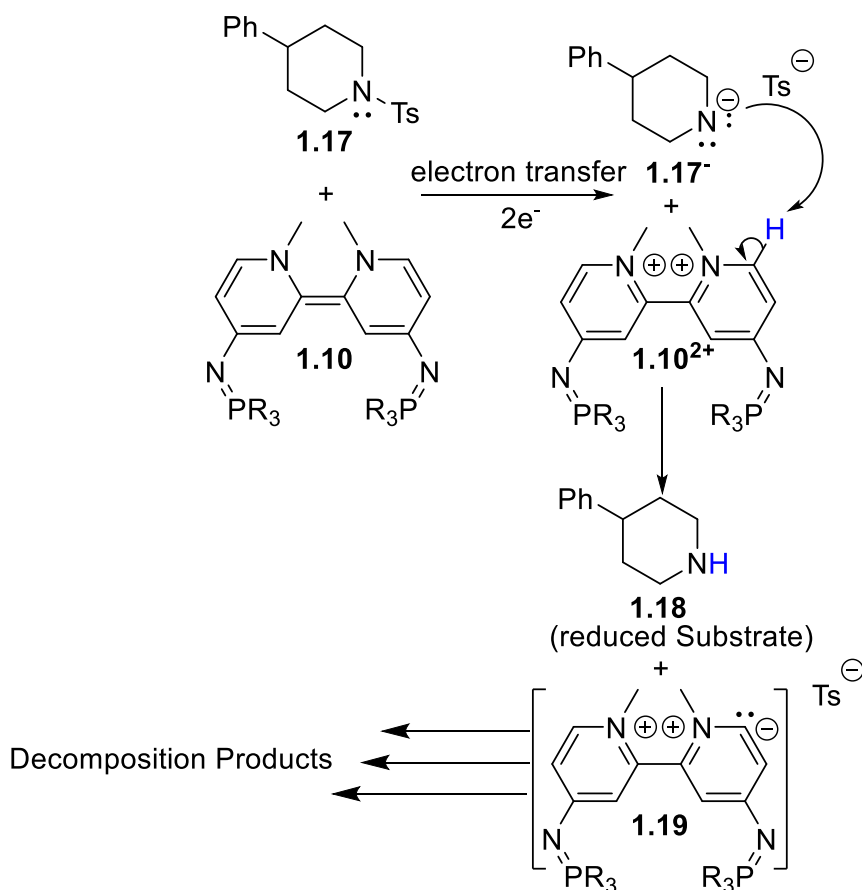


Scheme 1.6: Catalytic process using ORA **1.14** in a catalytic amount to reduce substrate $X-R_1$, forming product $H-R_2$.²⁷

The catalytic cycle is started by the addition of **1.15**, (0.2equiv.), sodium borohydride ($NaBH_4$ (2 equiv.)), dodecanethiol (dodecanethiol acts as a polarity reversal catalyst (PRC, 0.2 equiv.))^{28,29} and the substrate of choice (1 equiv.). $NaBH_4$ acts as a hydride source for compound **1.15**, converting it to the isolatable precursor (**1.13**) of the ORA (**1.14**). Oxygen then acts as an initiator for the first catalytic turnover,³⁰ performing the hydrogen abstraction from **1.13** to produce active ORA (**1.14**). The catalyst **1.14** then performs a single electron transfer to the substrate (R_1-X) and a fragmentation of the halide on the substrate occurs forming \dot{R}_1 and **1.15**, allowing for the catalytic cycle to be repeated (**Scheme 1.7**).²⁷ \dot{R}_1 naturally converts to the more stable radical species \dot{R}_2 which then performs the hydrogen atom abstraction in place of oxygen which is only needed as an initiator to the catalytic process, to give product (R_2-H) and **1.14**. After the first catalytic

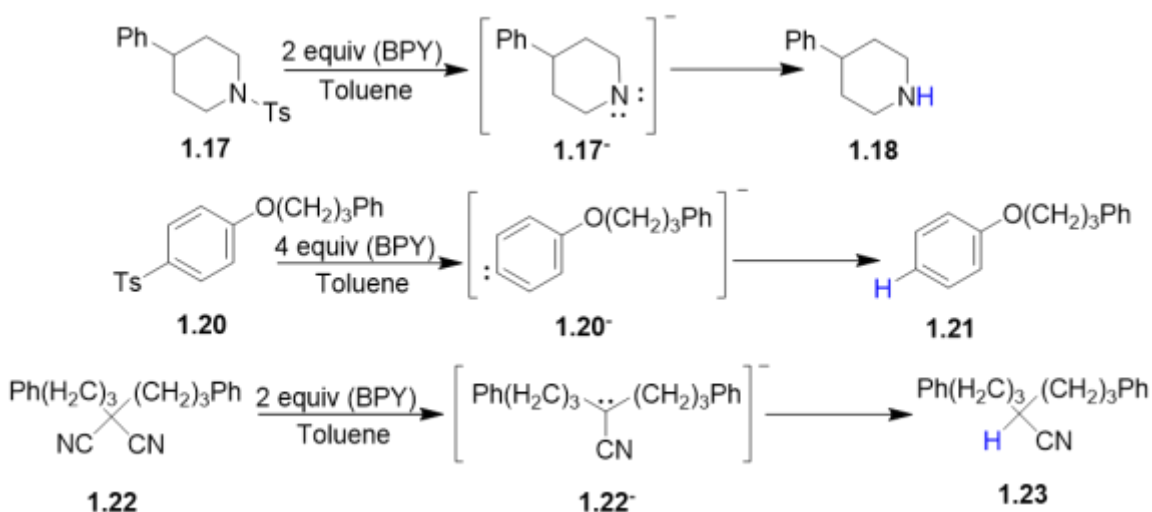
cycle is complete, PRC then helps to mediate the hydrogen atom abstraction of **1.13** with \dot{R}_2 , forming the ORA and increasing the speed of the overall catalytic cycle.²⁸ This cycle varies significantly from the catalytic cycle proposed in this study: however, it proved that it is possible to use ORAs in a catalytic manner.

Typically, substrates reduced by BPYs in a stoichiometric (non-catalytic) manner use the oxidized BPY species (for example **1.10**²⁺) as a proton source to generate the final product. It was proven through deuteration studies that it is the most acidic proton from the α carbon that is removed from the BPY²⁺ in order to generate product (**1.17**) from the unstable anionic intermediate (**1.16**).³¹ After **1.10**²⁺ is deprotonated the α -carbon becomes a highly reactive carbanion.³² This leads to **1.18** forming decomposition products (**Scheme 1.7**).³¹



Scheme 1.7: Protonation of anion intermediate from an oxidized BPY species.

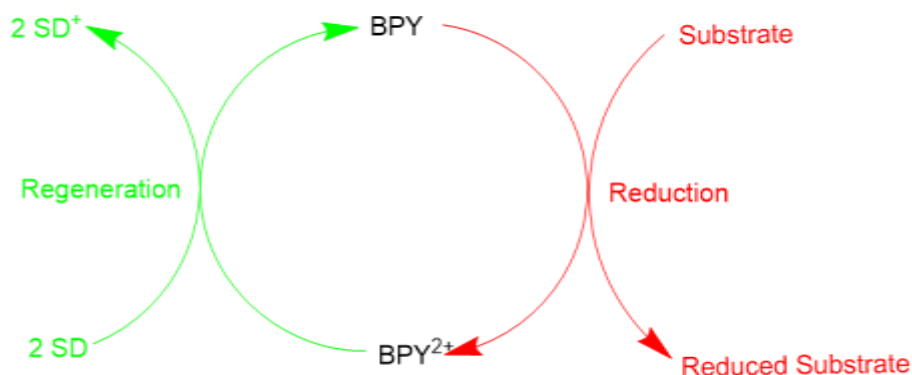
Ultimately this means that typical reductions that have been performed with BPYs such as the reduction of sulfones,² arenesulfonamides,³ triflamdes,⁶ acyloin derivatives,⁷ and Weinreb amides are not amenable to Murphy et al.'s catalytic process. This is because the reduction would form reactive anionic intermediates that deprotonate and decompose the BPY²⁺ species.²⁷ **Scheme 1.8** shows examples of various reductions facilitated by BPY derivatives, and the anionic intermediates that decompose the corresponding BPY²⁺ species.



Scheme 1.8: Typical reductions using BPY compounds.

Many BPY compounds have significantly larger molecular weights in comparison to the substrates they are reducing and an excess of BPY is often needed to achieve full reduction.^{15,33} This causes issues with purification of the reduced substrate due to the excess oxidized BPY and BPY related byproducts that are formed as a consequence of the reductions.³³ This in turn leads to higher overall cost to perform these reductions and decreased efficiency when using these reducing agents. The purpose of this study is the development of a catalytic cycle that uses a BPY derivative as a catalyst in the reduction

of various substrates, decreasing the overall cost, and increasing the overall efficiency, of reductions facilitated by BPY derivatives. (**Scheme 1.9**).



Scheme 1.9: Proposed catalytic cycle.

The proposed catalytic cycle is broken down into two separate half cycles, the first being the regeneration of the BPY from BPY²⁺. The second half of the catalytic cycle involves the reduction of the substrate using the chosen BPY. The key difference between the proposed catalytic cycle (**Scheme 1.9**) and the catalytic process developed by Murphy et al. (**Scheme 1.6**) is that the proposed catalytic cycle allows for two electron transfer systems as opposed to single electron transfer systems, allowing for different types of substrates to be reduced, and uses BPY derivatives as the ORA (catalytic species).²⁷ Unlike the catalytic process developed by Murphy et al. where there is a hydride, hydrogen, and electron transfer per cycle, only electrons are transferred through the proposed catalytic cycle. In depth detail of the potential and limitations of each half cycle and the overall proposed catalytic cycle are presented in Chapter 2: Results and Discussion.

Chapter 2: Catalytic Cycle Development and Substrate Testing

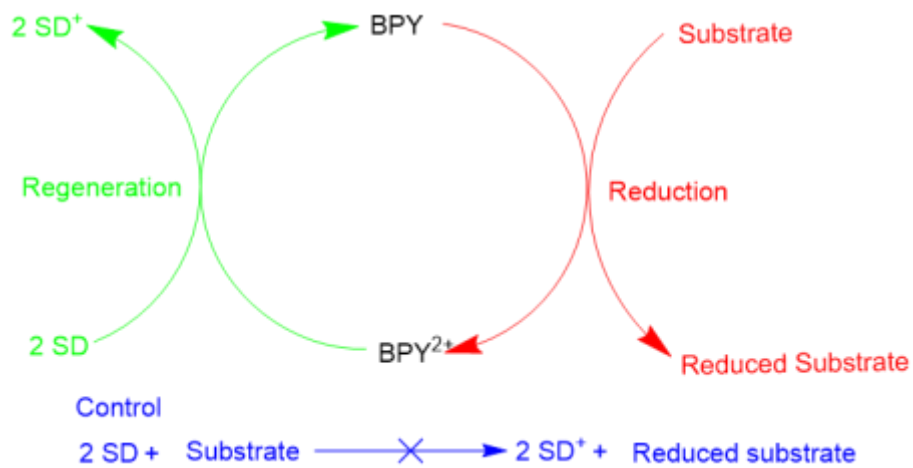
2.1: Introduction

Iminophosphorano substituted BPYs are among some of the strongest ORAs to date. They are highly tunable, with predicted reduction potentials that span from -1.14V to -2.12V vs SCE (calculations derived from various TEP values of different substituents).^{15,23,25} The large number of derivatives with different redox potentials should allow for BPY derivatives to be chosen for different applications based on their redox potentials and particular functional group selectivity.

The use of BPY compounds remains limited due to the fact that reactions typically require an excess of reducing agent and their large mass in comparison to the substrate they are reducing, which leads to excess byproduct,²⁵ purification issues, higher overall reaction cost and decreased efficiency of the overall reaction. In 2019 Murphy et al. developed a catalytic process that uses an ORA **1.14** as the catalyst (**Scheme 1.6**);²⁷ however, the method is not compatible with BPY derivatives as the ORA. This is because **1.14** is regenerated by reacting the singly oxidized **1.15** with a hydride followed by a loss of a hydrogen atom, while BPY derivatives are two electron donors, and BPY^{2+} is not known to be able to react with hydrides, therefore the BPY would not be regenerated by this protocol.

These issues led to the development of the catalytic cycle proposed herein that would allow for BPY compounds to act as a catalyst capable of donating two electrons in order to facilitate various reductions (**Scheme 2.1**). In order for this catalytic cycle to function, an adequate BPY derivative first needed to be chosen and synthesized, each stage

of the catalytic cycle needed be validated independently, and a control stage needed to be tested for each individual substrate to prove that the reduction proceeded via the ORA and not the sacrificial donor (**Scheme 2.1**). Once all of the above-mentioned steps were validated, then the catalytic cycle could be optimized for various substrates.

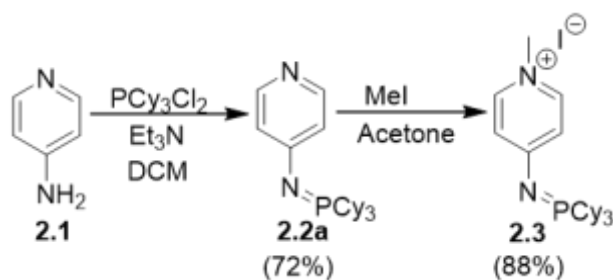


Scheme 2.1: Proposed catalytic cycle and control stage.

2.2: Results and Discussion

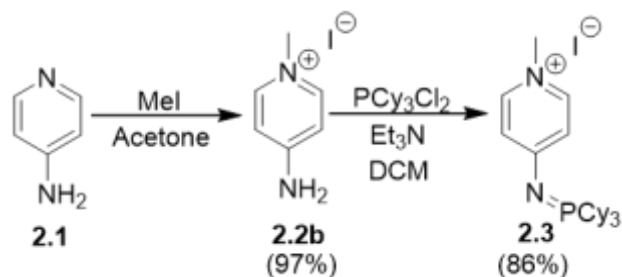
Choosing and synthesizing a suitable BPY was the first goal that needed to be accomplished in this study. A BPY derivative with a low redox potential was desired to allow for the reduction of a large variety of substrates and generally faster reductions. It was decided that an di-iminophosphorano substituted BPY would be used instead of a tetra-substituted BPY. This is because di-substituted BPYs are more stable, easier to prepare and still offer low redox potentials.²⁶ Both the BPY and its oxidized species must be stable, and stable in the presence of one another, as both will be present in the reaction mixture at the same time throughout the duration of the catalytic cycle. BPY **1.12** was chosen as it is synthetically easy to make, has a high solubility in organic solvents, and its presence, and the presence of its oxidized counterpart can be monitored throughout the catalytic cycle through the use of phosphorous nuclear magnetic resonance spectroscopy (³¹P NMR), simplifying monitoring of the overall catalytic cycle. Furthermore, **1.12** is a stronger reducing agent than the similar di-substituted triphenyliminophosphorano derivative (BPY **1.10b**, -1.34V vs SCE) and it is among the strongest di-substituted derivatives prepared to date.

A new synthetic route was proposed for the synthesis of **2.3**, which is the direct precursor to BPY **1.12**. Compound **2.3** had previously been synthesized by Hanson,¹¹ however this synthetic pathway was not optimized (**Scheme 2.2**).



Scheme 2.2: Formation of **2.3** following Hanson's synthetic pathway.

In **Scheme 2.2** dichlorotricyclohexylphosphorane (Cl_2PCy_3) acts as a source of the PCy_3 unit in **2a** and **2.3**, and triethylamine (Et_3N) acts as a base. The NH_2 group on the 4-aminopyridine undergoes nucleophilic attack of the Lewis acidic phosphorous center, while NEt_3 pushes the reaction forward by removing HCl to form $\text{Et}_3\text{NH}^+\text{Cl}^-$ leading to the formation of pyridinium **2.2a**. Compound **2.2a** is then methylated, yielding compound **2.3**. More recently Dyker et al. was able to develop a more practical synthetic method for iminophosphorano substituted pyridinium ions similar to **2.3**, including a series of BPY precursor compounds that could be used to create tetrasubstituted BPYs.³³ The synthetic method developed by Dyker et al. was used to increase the cost efficiency of the overall synthesis. This was done by performing the nucleophilic addition of the methyl group to 4-aminopyridine prior to the dehydrohalide coupling³⁴ of the PCy_3 unit, which comes from the more costly, air and moisture sensitive reagent (Cl_2PCy_3) **Scheme 2.3**. Using the more expensive/sensitive reagent last avoids loss during the multistep reaction.



Scheme 2.3: Improved synthetic pathway for the formation of **2.3**.

It was shown in this study that the BPY precursor to **1.12** could be produced in good yield following the same synthetic pathway (**Scheme 2.3**). The yields of each reaction step were also increased when using this method. The yield of the methylation step increased from 88% to 97% and the yield of the N=PCy₃ bond formation increased from 72% to 86% (**Scheme 2.2/2.3**). The pyridinium ion **2.3** prepared by this route showed high purity through both ³¹P NMR spectroscopy (**Figure 2.1**, singlet at 35.7 ppm, which corresponds to the literature value at 36.2 ppm)¹¹ and proton NMR spectroscopy (¹H NMR, **Figure 2.2**), which corresponds to the literature spectrum and shows no impurities.

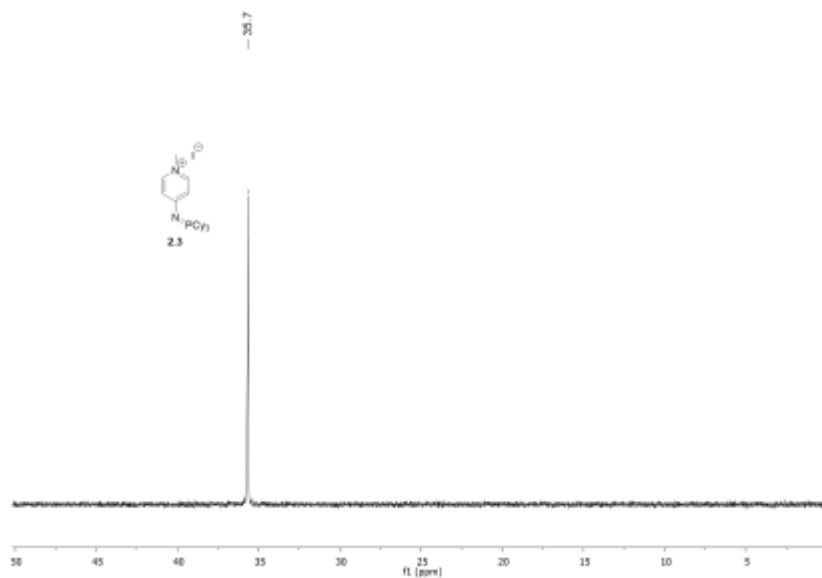


Figure 2.1: ³¹P NMR spectrum of compound **2.3** in CDCl₃.

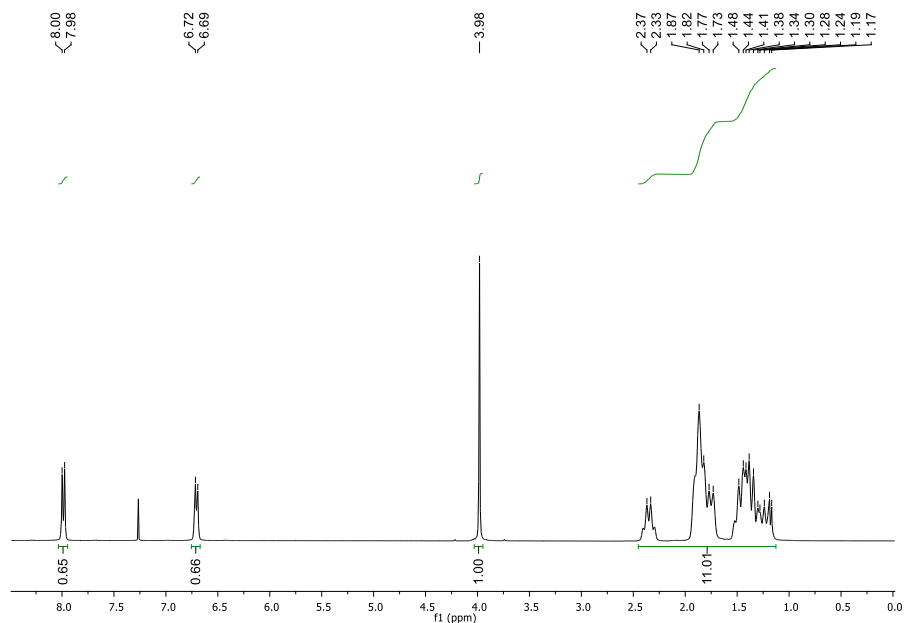
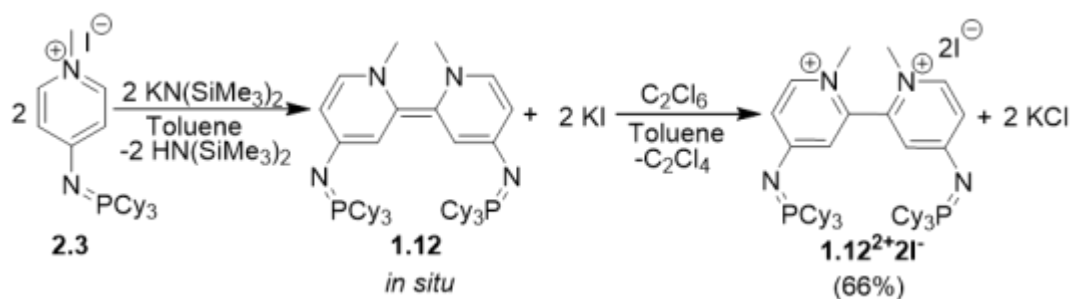


Figure 2.2: ^1H NMR spectrum of compound **2.3** in CDCl_3 .

BPY derivatives are air and moisture sensitive and can be difficult to isolate in high yields. Isolated BPY **1.12** is not needed for the regeneration stage or the control stage and could be generated *in situ* from the BPY precursor for the reduction stage. On the other hand, isolated and pure $\mathbf{1.12}^{2+}2\mathbf{I}^-$ was needed to test whether or not it could be reduced back to BPY **1.12** effectively in the regeneration stage. Ultimately using $\mathbf{1.12}^{2+}2\mathbf{I}^-$ as the starting material for the catalytic cycle would also simplify catalytic loading as it is not air and moisture sensitive and has a significantly longer shelf life than its BPY counterpart. For these reasons a modified procedure was developed where the BPY is not isolated but instead is oxidized *in situ* to produce $\mathbf{1.12}^{2+}2\mathbf{I}^-$ (Scheme 2.4). Following the successful formation of the BPY **1.12** by deprotonation of **2.3** with $\text{KN}(\text{SiMe}_3)_2$, hexachloroethane was added directly to the mixture and the oxidized BPY ($\mathbf{1.12}^{2+}2\mathbf{I}^-$) was isolated in a moderately good yield of 66%. Bipyridinium $\mathbf{1.12}^{2+}2\mathbf{I}^-$ also showed high purity through both ^{31}P NMR spectroscopy (Figure 2.3, singlet at 38.4 ppm, which corresponds to the

literature value at 37.7 ppm) and ^1H NMR spectroscopy (**Figure 2.4**) which corresponds to the literature spectrum.



Scheme 2.4: Synthetic pathway for the formation of BPY $1.12^{2+}2\text{I}^-$.

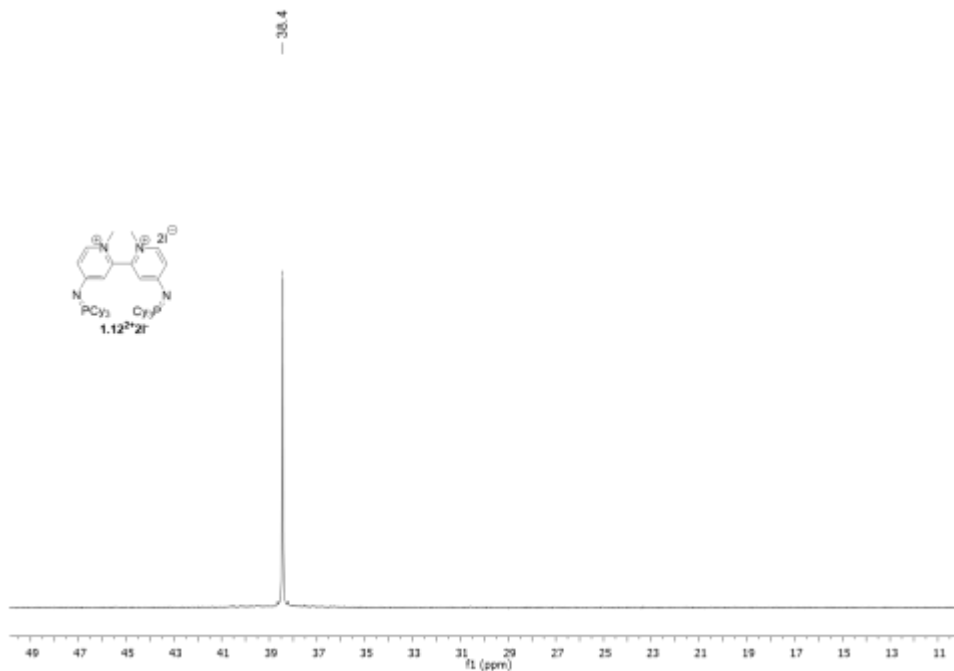


Figure 2.3: ^{31}P spectrum of compound $1.12^{2+}2\text{I}^-$ in CDCl_3 .

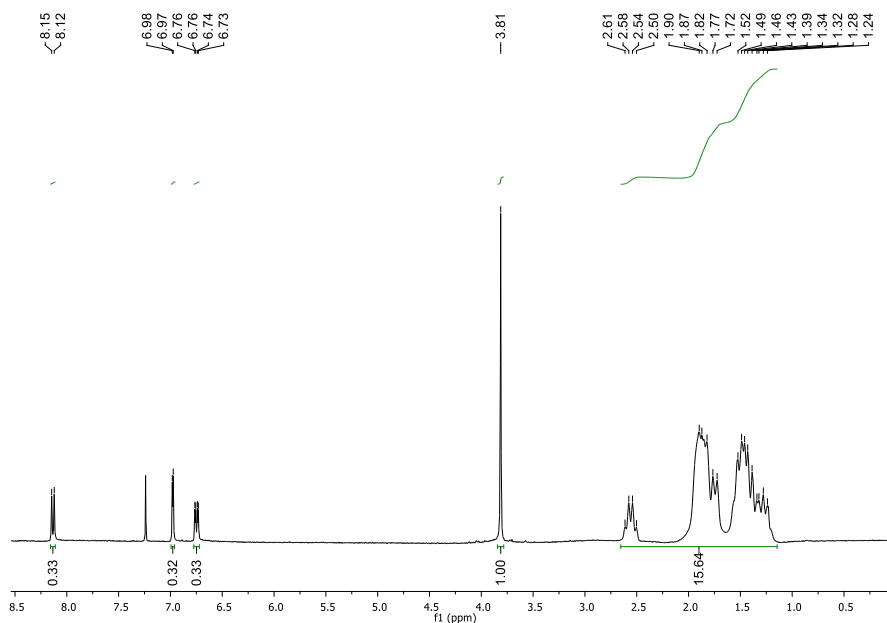
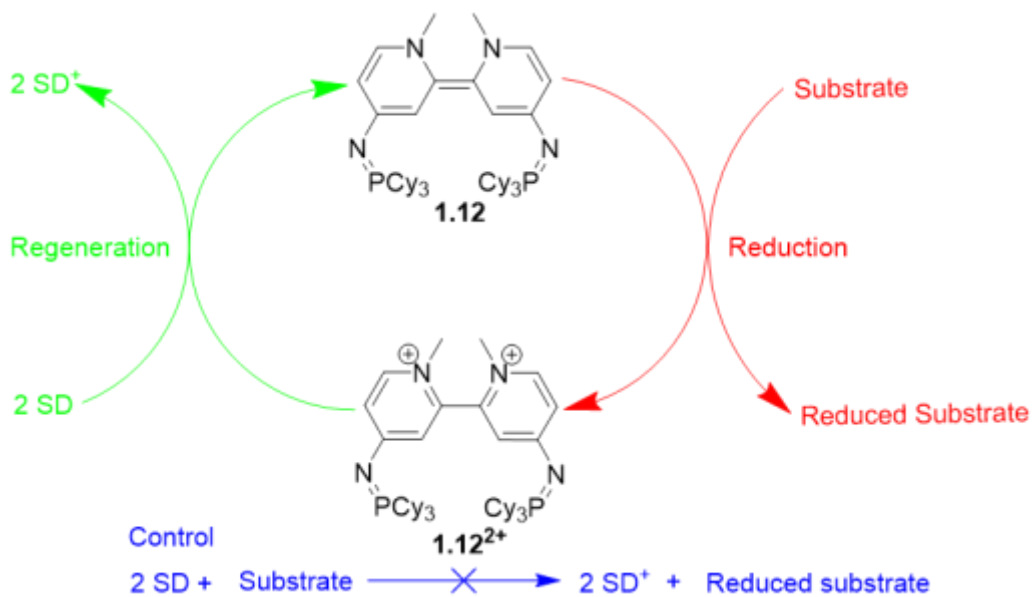


Figure 2.4: ^1H NMR spectrum of compound $\mathbf{1.12}^{2+}2\text{I}^-$ in CDCl_3 .

With the isolation of pure oxidized BPY $\mathbf{1.12}^{2+}2\text{I}^-$, the efficacy of potential sacrificial donors for the regeneration step (forming $\mathbf{1.12}$ from $\mathbf{1.12}^{2+}$) of the proposed cycle could be tested (**Scheme 2.5**).



Scheme 2.5: Catalytic cycle with chosen BPY $\mathbf{1.12}$.

In order for **1.12** to be regenerated, **1.12²⁺** needs to be reduced through the use of a sacrificial donor (SD), which must be a stronger reducing agent than **1.12**. The reduction of **1.12²⁺** via the chosen SD also needs to be quicker than the analogous reduction of the substrate. For these reasons, magnesium and a series of alkali metals were assessed as potential SD for the regeneration stage of the catalytic cycle (**Table 2.1**).

Table 2.1: Sacrificial donors tested for use in the regeneration stage.

Metal (SD)	Solvent	Duration of reaction, % of 1.12²⁺ converted to 1.12 /byproducts
2 Li (-3.04V vs. SCE)	Benzene	15h 0% conversion
	THF	23.5h 0% conversion
2 K (-2.93V vs. SCE)	Benzene	3.5h Full conversion, many impurities
	THF	2h Full conversion, many impurities
Mg (-2.37V vs. SCE)	Benzene	Not attempted
	THF	2.5 days 0% conversion
<u>2 Na</u> (-2.71V vs. SCE)	Benzene	15.5h 0% conversion
	<u>THF</u>	<u>13h</u> <u>100% conversion, no impurities</u>

As seen in **Table 2.1**, four different metals were tested as potential sacrificial donors, in benzene and/or THF solvents. Each test reaction was performed with 1 equivalent of **1.12²⁺2I⁻**, and 40 equivalents of the SD. The large excess of SD was used in anticipation of the full catalytic cycle; the excess SD allows for the catalytic BPY to be regenerated indefinitely until full reduction of the substrate occurs. Each metal had its passivation layer³⁵ manually removed prior to the corresponding test reactions. No reduction was observed through ³¹P NMR spectroscopy when using lithium (Li, **Figure A3**) or magnesium (Mg, **Figure A4**) as the sacrificial donor. **1.12²⁺2I⁻** appeared to be more soluble in THF than benzene and no reduction occurred when attempting the reduction using magnesium and THF, therefore, the reduction was not attempted in benzene. The trials using potassium (K) showed good reaction times as all the starting material was consumed within the first hour when the reduction was attempted in both solvents. The reduction was complete in two hours as determined through ³¹P NMR spectroscopy in THF and 3.5h in benzene. The trials were not successful however since many impurities were formed during the reactions as indicated by unexpected peaks observed through ³¹P NMR spectroscopy (**Figure A5**). This is not optimal as the trials represent one half cycle, meaning that with lower catalytic loading during the overall catalytic cycle, a larger amount of impurities would likely be formed, as the regeneration stage occurs multiple times. This would ultimately decrease the purity and overall yield of the reduced substrate. Sodium (Na) was unable to reduce **1.12²⁺2I⁻** in benzene. The reaction was monitored through ³¹P NMR spectroscopy for 15.5h at which point it was abandoned. No BPY was observed in the ³¹P NMR spectra, and the peak representative of the starting material (**1.12²⁺**) had a low

intensity. This is likely due to the poor solubility of **1.12**²⁺ in benzene. Reduction did however occur when THF was used as the solvent and sodium was used as a SD (**Figure 2.5**). When using sodium metal as a SD, the reaction rate was slower than when compared to K; however, no impurities were observed.

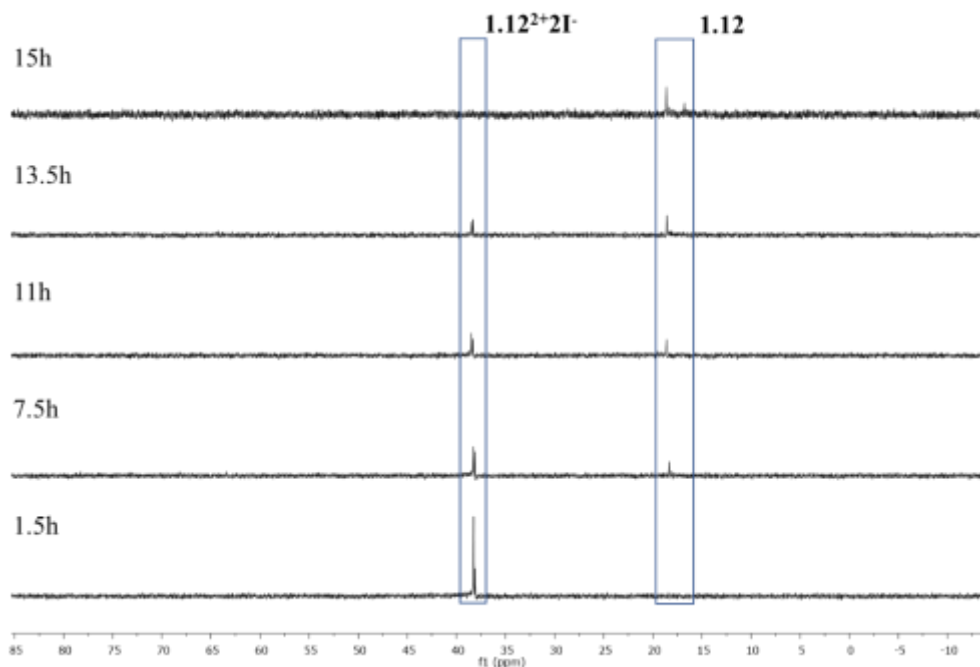


Figure 2.5: Stacked ³¹P NMR spectra, monitoring the reduction of **1.12**²⁺**2I**⁻ via Na in THF over 15 hours.

Figure 2.5 shows one of the three trials conducted where Na was used as a SD in order to reduce **1.12**²⁺**2I**⁻ in THF. This trial was monitored through ³¹P NMR spectroscopy and the reduction was complete in 15h. All of **1.12**²⁺**2I**⁻ (38.4ppm) was converted to **1.12** which is known to occur as two stereoisomers¹¹ (16.8ppm and, 18.6ppm for *Z* and *E* isomer respectively: see **Figure 2.6**), with no impurities. When forming **1.12** from its precursor **2.3**, the *Z* isomer is the major isomer however, it was observed here that when forming

1.12 from **1.12**²⁺**2I**⁻ via Na that the *E* isomer is the major isomer. It should be noted that the isomers are inseparable and demonstrate the same electrochemical characteristics.¹¹

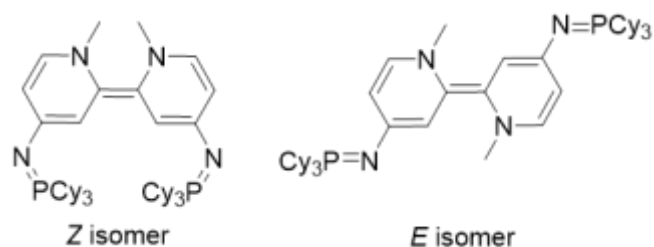
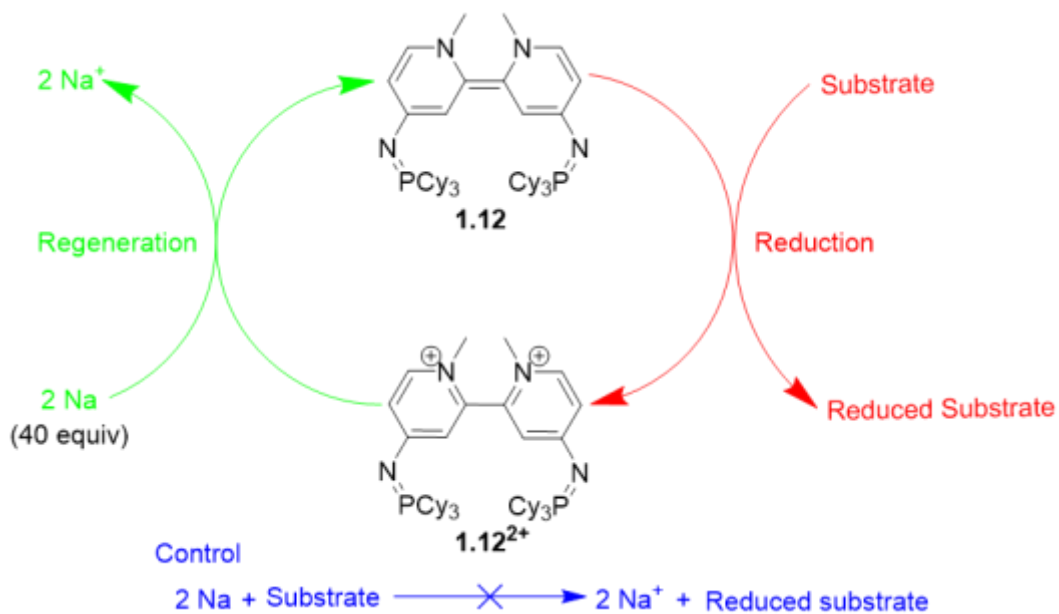


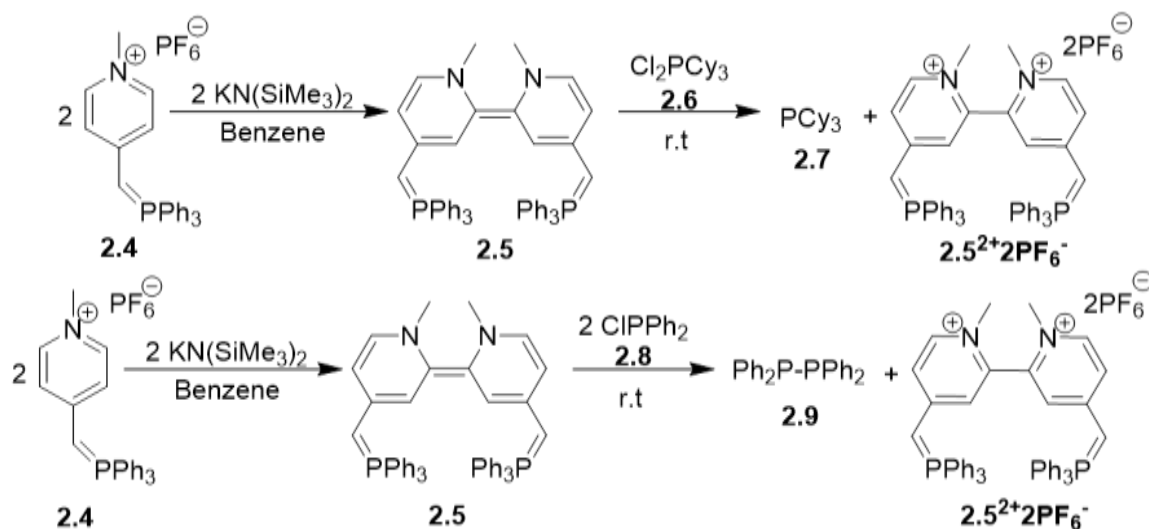
Figure 2.6: Z and E isomers of **1.12**.

Sodium was tested as a SD three times in THF and the average reaction time is reported in **Table 2.1**. The reaction rates averaged over all three trials using THF are very similar (15h, 12h, 12.5h) and no impurities were observed in all three trials, making sodium the most promising SD that was tested, and THF the most promising solvent (**Scheme 2.6**).



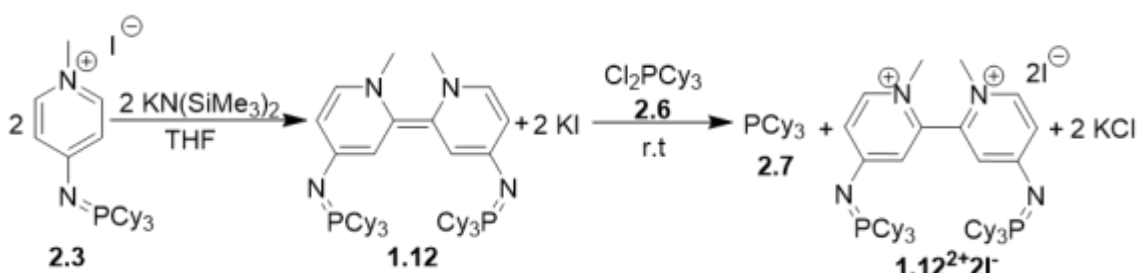
Scheme 2.6: Catalytic cycle with chosen BPY (**1.12**) and SD (Na).

The second half of the catalytic cycle involves the reduction of the substrate through the use of BPY **1.12** (**Scheme 2.6**). In order for this half cycle to be a success, **1.12** must be able to reduce the substrate into stable anions that are not strong bases, so as to avoid the deprotonation/decomposition of **1.12**²⁺ (which would make regeneration of **1.12** impossible as discussed in **Scheme 1.7**). Potential substrates for this catalytic cycle would include, but not be limited to various halogenated phosphoranes. It has previously been demonstrated that halogenated phosphoranes can be reduced by BPY derivatives, generating BPY²⁺ as a stoichiometric byproduct (**Scheme 2.7**).⁵ Using halogenated phosphoranes would also allow for the monitorization of the reduction of the substrate to product through ³¹P NMR spectroscopy, similar to **1.12** and **1.12**²⁺.³⁶ **Scheme 2.7** shows the successful reduction of both dichlorotricyclohexylphosphorane (**2.6**) and chlorodiphenylphosphine (**2.8**) using BPY **2.5** as the reducing agent at room temperature.⁵



Scheme 2.7: Reduction of halogenated phosphoranes using BPY **2.5**.⁵

BPY **2.5** and byproduct KPF_6 are formed through the reaction of **2.4** with $\text{KN}(\text{SiMe}_3)_2$. The substrate is then added to the reaction mixture allowing for its reduction and the formation of the oxidized BPY $\mathbf{2.5}^{2+}\mathbf{2PF}_6^-$. The initially formed chloride anion undergoes a metathesis with the KPF_6 present from the formation of the BPY to produce KCl and $\mathbf{2.5}^{2+}$ as a PF_6^- salt. It was decided that substrate **2.6** would be the first to be tested in the reduction stage (**Scheme 2.8**), to confirm that it is possible to reduce the substrate using **1.12** in THF and to allow for an assessment of the reaction rate.



Scheme 2.8: Reduction of dichlorotricyclohexylphosphorane **2.6** to phosphine **2.7** through the use of **1.12** (formed *in situ*).

Similar to the literature, the reduction of **2.6** was done using 1 equiv. of the BPY **1.12** which was generated *in situ* from the pyridinium precursor **2.3**. The substrate was then added directly to the reaction mixture and the reaction was complete after 10 minutes as proven through ^{31}P NMR spectroscopy. **Figure 2.7** shows the ^{31}P NMR spectrum representing the reduction of **2.6** using BPY **1.12**. The NMR spectrum was acquired 10 minutes after the substrate is added to the reaction mixture containing **1.12** (generated *in situ*). It shows that all of **2.6** (97.8 ppm) had reacted, with 94% (based on ^{31}P NMR spectroscopy integrations) converted to the reduced phosphine product **2.7** (10.9 ppm),⁵ and 6% converted to phosphine oxide (OPCy_3 (45.6 ppm)).

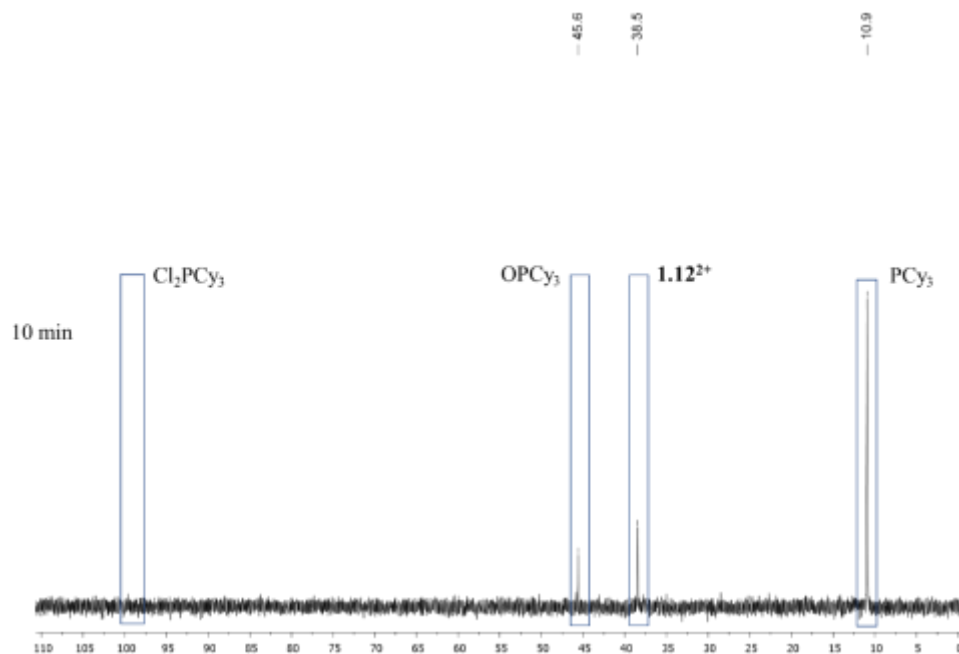
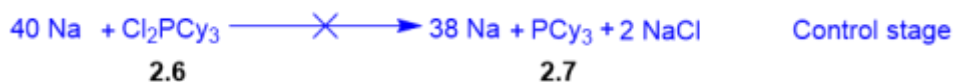


Figure 2.7: ^{31}P NMR spectrum of the reaction mixture of the reduction of **2.6** in THF via BPY **1.12** (generated in situ) after 10 minutes.

The formation of the phosphine oxide was likely due to the hydrolysis of the dichlorophosphorane **2.6** by residual water in the THF. The presence of the $\mathbf{1.12}^{2+}\mathbf{2I}^-$ is also seen at 38.5 ppm, consistent with **Figure 2.3**. These results were promising, as the reduction occurred fast; however, before a complete catalytic cycle could be attempted a control test still needed to be performed (**Scheme 2.9**). This would determine the base rate for the reduction of **2.6** by the sacrificial donor sodium. Ideally this reaction would not

proceed at all, or would be very slow, so that any rate enhancement by catalytic amounts of BPY is easily apparent.



Scheme 2.9: Control test for the reduction of **2.6** with sodium.

Halogenated phosphoranes have been reported to react sluggishly with metals³⁷ yet quickly with BPYs.⁵ This proved beneficial to the success of both the reduction stage and the control stage. **Figure 2.8** shows the attempted reduction of **2.6** via Na monitored over 18h.

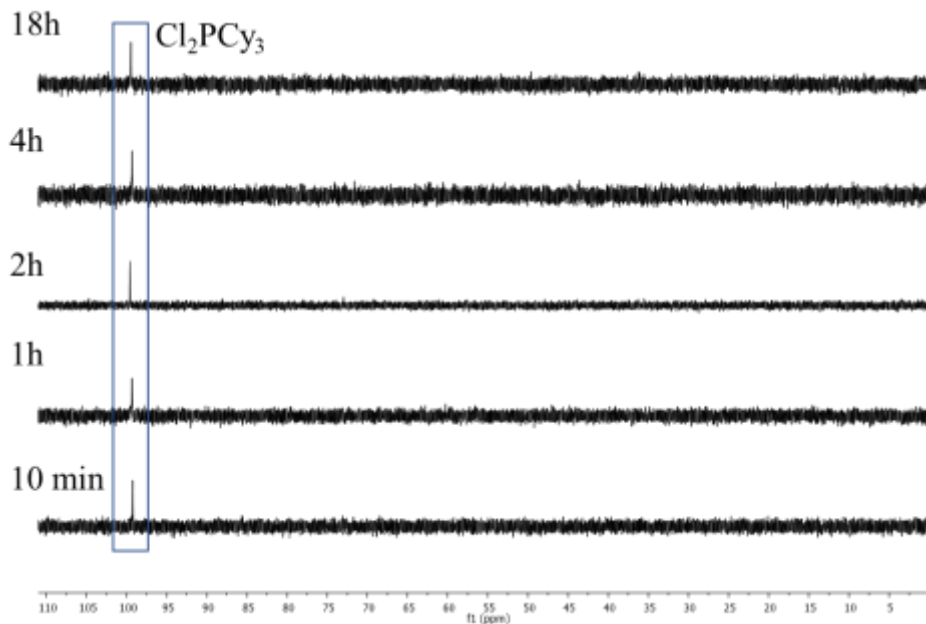
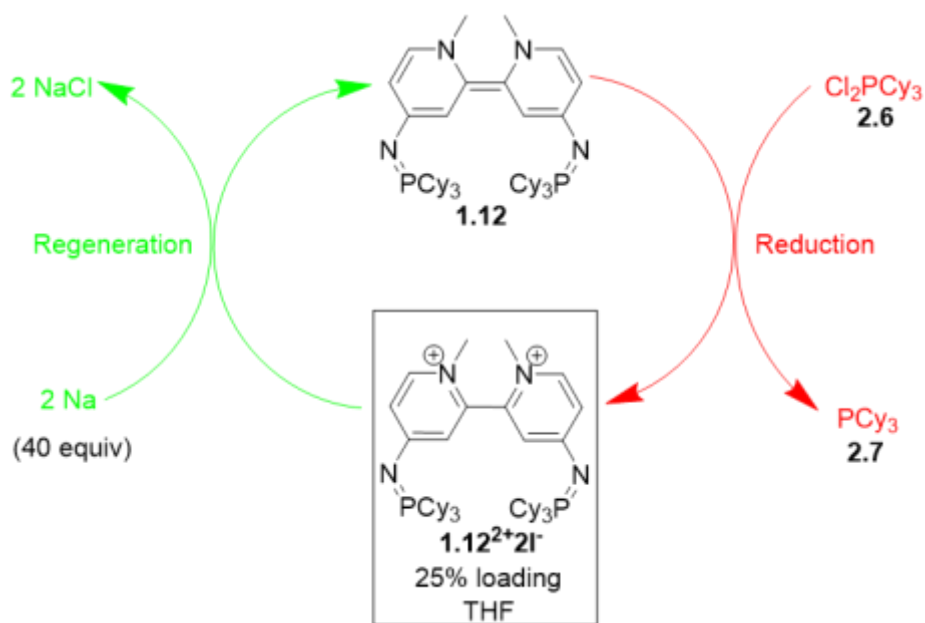


Figure 2.8: Stacked ³¹P NMR spectra, monitoring the reduction of **2.6** via Na in THF over 18h.

Similar to the regeneration stage, 40 equivalents of Na were used to attempt to reduce the substrate. After 18 hours ³¹P NMR analysis of the reaction mixture showed no signal for Cy₃P (10.9 ppm) indicating that no reduction had occurred, and only starting

material was visible (97.8ppm). The control test was repeated to ensure that Na was unable to reduce **2.6** and the results were the same for both trials. The BPY could be regenerated from sodium and BPY²⁺ (regeneration stage), the BPY could also reduce **2.6** quickly (reduction stage) and sodium was unable to effectively reduce the substrate (control stage). With all stages proving successful individually the full catalytic cycle could now be tested (Scheme 2.10).



Scheme 2.10: Full catalytic cycle showing all chosen species

Substrate **2.6** (1 equiv.) was added to 4mL of THF, along with **1.12²⁺** (0.25 equiv.), and finally sodium (40 equiv.) was added to the reaction mixture. The reaction was then monitored over three days by ³¹P NMR spectroscopy for any indication of substrate reduction (**Figure 2.9**).

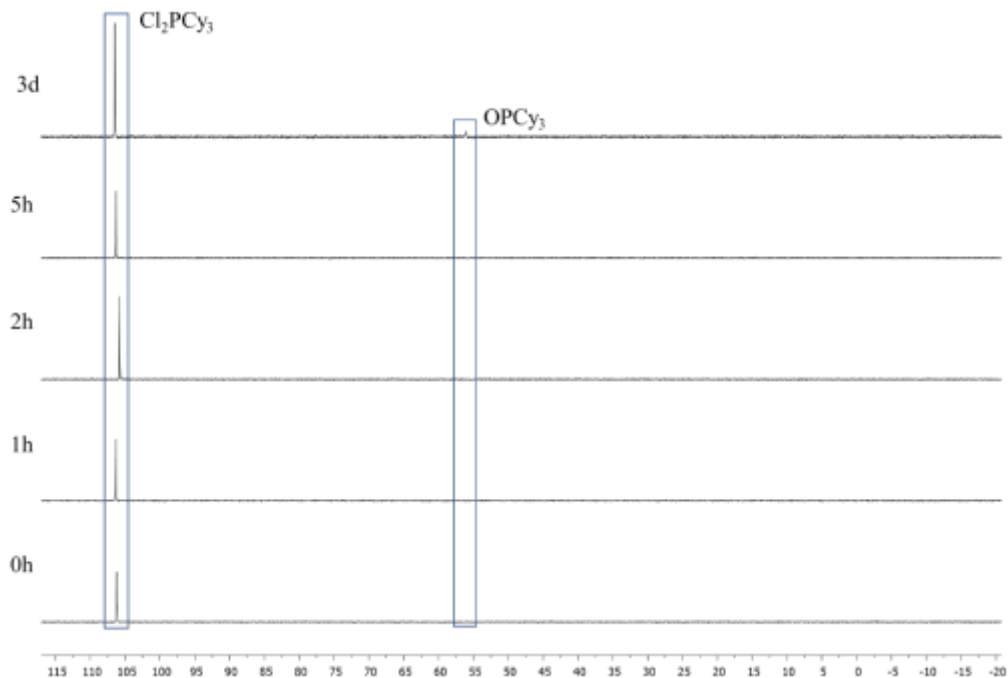
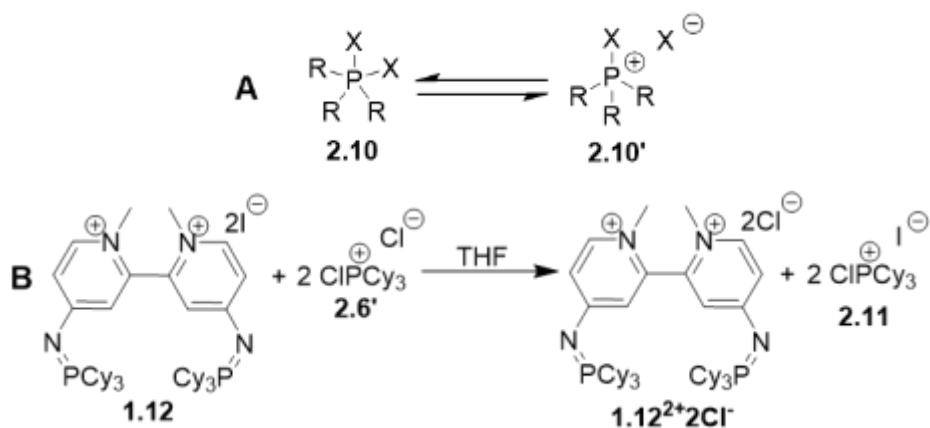


Figure 2.9: Stacked ^{31}P NMR spectra monitoring the reduction of **2.6** with 25 eq of **1.12 $^{2+}$** and 40 eq of Na in THF.

Unfortunately, after three days no reduction occurred, and the catalytic cycle attempt was unsuccessful. It can also be seen that only the substrate dissolved into solution (106.3ppm) and unexpectedly no phosphorous signals for **1.12 $^{2+}$** were observed, indicating that it remained undissolved in the reaction mixture. Since earlier work on the reduction stage indicated that **1.12 $^{2+}2\text{I}^-$** was sufficiently soluble, this finding is likely due to the presence of the substrate causing a metathesis reaction^{38,39} to occur and produce an insoluble dichloride salt of the oxidized BPY (**1.12 $^{2+}2\text{Cl}^-$** , **Scheme 2.11B**).

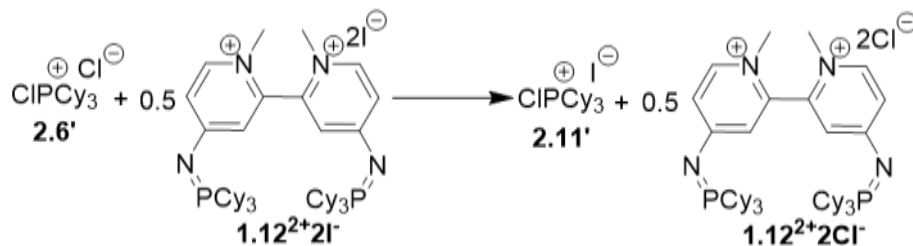


Scheme 2.11: **A:** equilibrium between pentavalent and tetravalent geometry in phosphoranes. **B:** Metathesis of **2.6'** with **1.12²⁺2I⁻**.

As can be seen in **Figures 2.8/2.9**, the chemical shift representative of dichlorotriphenylphosphorane (**2.6**) is reported as a different value (97.8 ppm, and 106.3 ppm respectively). In each instance there was a different amount of iodide present in the reaction mixture. The overall geometry of a compound can largely affect its chemical shift determined through ³¹P NMR spectroscopy. When phosphorane **2.6** is dissolved in THF its equilibrium is shifted from the pentacoordinate species (which is the predominate species present in solid state)⁴⁰ towards the more favorable tetra-coordinate phosphonium species (**Scheme 2.11 A**). The more polar the solvent is the greater the shift in the equilibrium towards the tetra-coordinate species is, and the further downfield the chemical shift will appear (compared to its pentacoordinate isomer).⁴⁰

Since THF is consistently used as the solvent, it was not likely that solvent effects alone were altering the chemical shift of **2.6**. It was also thought that when phosphonium **2.6** is in the presence of **1.12²⁺2I⁻** a metathesis reaction occurs (**Scheme 2.11 B**) which would form the insoluble dichloride salt (**1.12²⁺2Cl⁻**) that would precipitate out of solution.

In order to verify what was causing the discrepancy in the chemical shift of **2.6** and to determine if the metatheses of **1.12²⁺2I⁻** and **2.6** was occurring, the two compounds were mixed together in THF in an attempt to force the metathesis reaction to occur (**Scheme 2.12**).



Scheme 2.12: Metathesis reaction between **2.6'** and varying equivalents of **1.12²⁺2I⁻**.

Upon reacting **2.6'** with 0.5 equivalents of **1.12²⁺2I⁻** the expected product was **2.11'**. Phosphonium **2.6'** and phosphonium **2.11'** should have the same chemical shift since the CIPCy_3^+ cation should give the same chemical shift irrespective of the counter anion.⁴¹ The presence of **1.12²⁺2I⁻** determined through ³¹P NMR spectroscopy acts as an indication as to whether or not the metathesis reaction has proceeded since **1.12²⁺2Cl⁻** is insoluble in THF. **Figure 2.10** shows that the peak representing **2.6** is clearly being shifted further downfield upon the addition of **1.12²⁺2I⁻**. Before the addition of **1.12²⁺2I⁻**, substrate **2.6** has a chemical shift of 99.3 ppm. This chemical shift represents what was seen in the control test (97.8 ppm, **Figure 2.8**), when there was no iodide source present in the reaction mixture. The poor solubility of **2.6** in THF can be seen by the signal to noise ratio (bottom spectrum, **Figure 2.10**). Once 0.5 equivalents of **1.12²⁺2I⁻** is added (top spectrum, **Figure 2.10**) the chemical shift of **2.6** appears at 106.4 ppm, a small amount of tricyclohexylphosphine oxide (OPCy_3) can be seen at 45.8 ppm, and there is no peak representative of oxidized BPY (**1.12²⁺**) detected by ³¹P NMR spectroscopy. This indicates that **1.12²⁺2I⁻** did undergo

a metathesis reaction with **2.6** and precipitated out of solution as a dichloride salt (precipitation was also observed in the reaction mixture). These results are also comparable to the results of the previous full catalytic cycle attempt which had 0.25 equivalents of **1.12²⁺2I⁻** and only showed a chemical shift for the substrate at 106.3 ppm through ³¹P NMR spectroscopy (**Figure 2.9**). With an increase of iodide in the reaction mixture the chemical shift of the substrate is moved further downfield. These results indicate that when iodide is present in the reaction mixture the equilibrium of the substrate shifts closer to the tetracoordinate species; and by increasing the amount of iodide, the chemical shift of the substrate is shifted further downfield.⁴¹ To further support this, one equivalent of iodine and one equivalent of **2.6** were mixed together in THF. The chemical shift visible through ³¹P NMR spectroscopy of **2.6** appeared at 108.2 ppm (see appendix **Figure A6**).

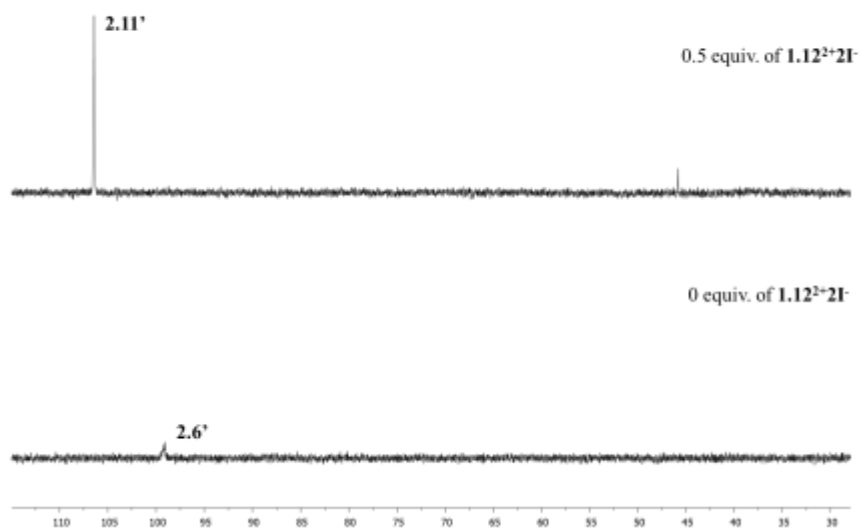
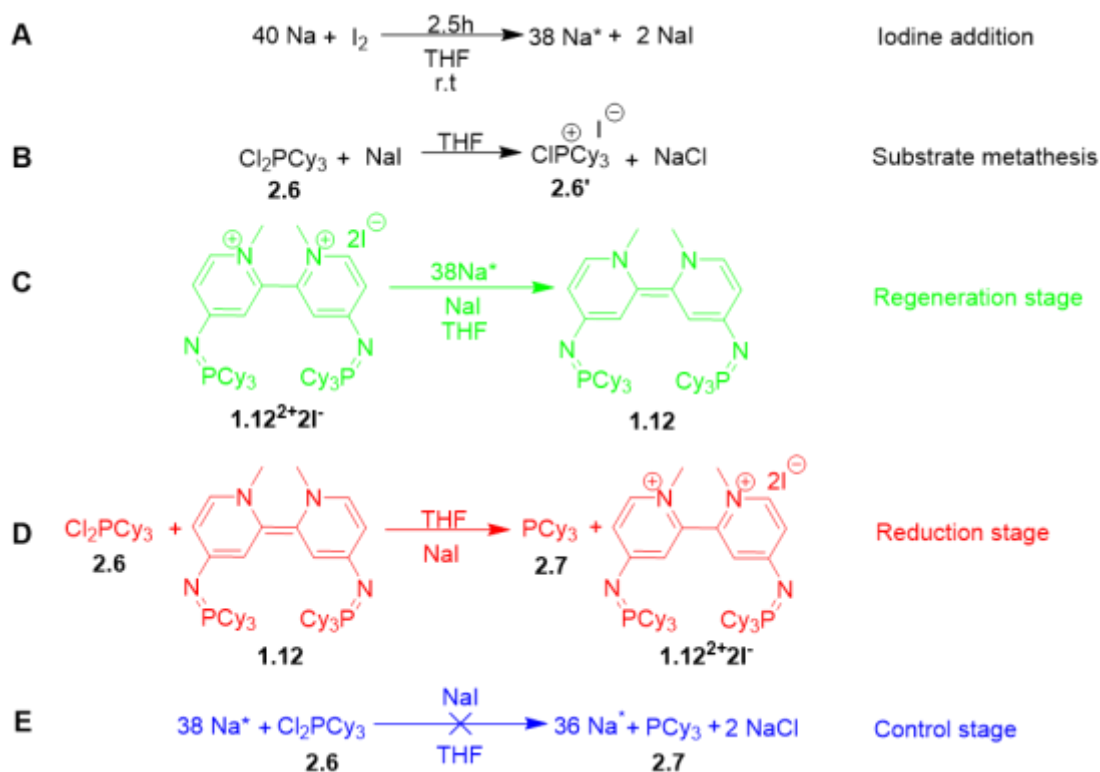


Figure 2.10: Metathesis reaction between **2.6** and 0.5eq of **1.12²⁺2I⁻**.

This experiment and its relation to the previous experiments involving substrate **2.6** provide strong evidence that a metathesis reaction is likely occurring between **2.6** and **1.12²⁺2I⁻**. Since oxidized BPY (**1.12²⁺2Cl⁻**) is insoluble in THF, it cannot be reduced by sodium through a surface area reaction. This meant that moving forward, an excess of iodide would be needed to be used in order to prevent the metathesis between **2.6** and **1.12²⁺2I⁻** and to prevent the precipitation of **1.12²⁺** as a dichloride salt. It was decided that the simplest way to add a source of iodide would be to use iodine (I₂) as it is soluble in THF (**Scheme 2.13A**).

By adding an equivalent of iodine prior to the catalytic cycle, an abundance of sodium iodide is created (**Scheme 2.13A**) which will undergo metathesis with **2.6** (**Scheme 2.13B**). This metathesis reaction is more favorable than the reaction between **2.6** and **1.12²⁺2I⁻** therefore preventing the formation of the insoluble salt **1.12²⁺2Cl⁻**. **Scheme 2.13** shows how the addition of iodine affects each individual stage of the catalytic cycle.



Scheme 2.13: Iodine addition and its effects on each stage of the catalytic cycle.

Iodine was added to sodium in THF followed by stirring until the dark color completely dissipated (2.5h), indicating that all of the iodine had reacted with the sodium. By reacting iodine with sodium, the sodium was also chemically activated making it more reactive (activated sodium is represented by Na^* (**Scheme 2.13**)), allowing $\text{1.12}^{2+}2\text{I}^-$ to be reduced more quickly (**Scheme 2.13C/Figure 2.11**).

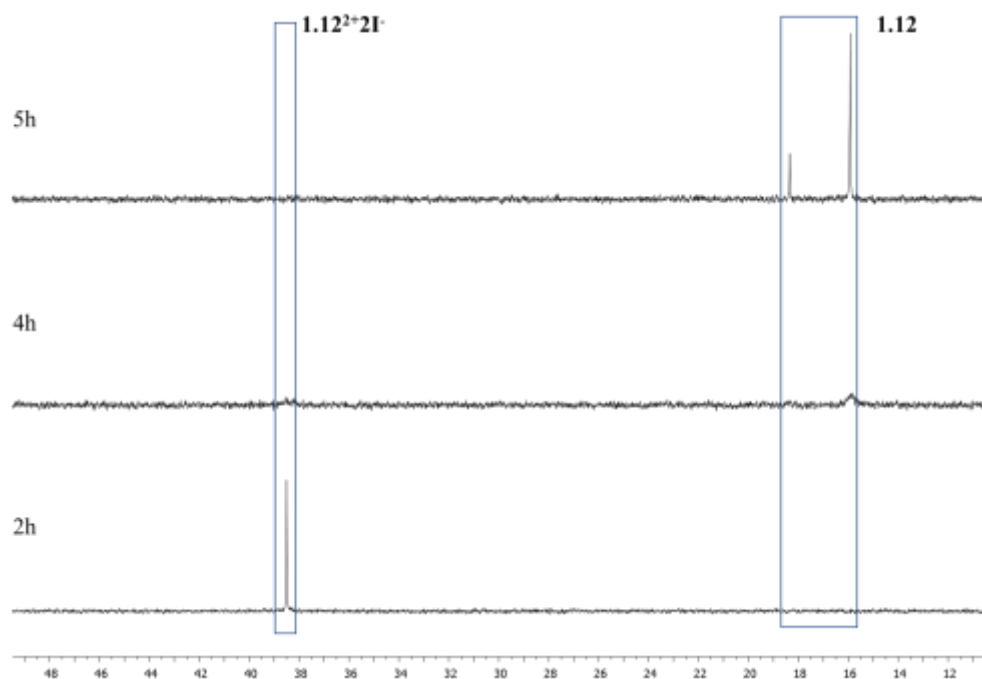


Figure 2.11: Stacked ^{31}P NMR spectra, monitoring the reduction of $\mathbf{1.12}^{2+}2\mathbf{I}^-$ via Na^* in THF.

The time required to reduce $\mathbf{1.12}^{2+}2\mathbf{I}^-$ with Na^* averaged over 3 trials, was 3.7h (with the slowest run shown in **Figure 2.11**). As can be seen above, 2 hours after the addition of $\mathbf{1.12}^{2+}2\mathbf{I}^-$ there was no change and no signs of reduction however, after 5 hours all of $\mathbf{1.12}^{2+}2\mathbf{I}^-$ had been reduced to BPY **1.12** (18.5 ppm, 15.7 ppm) with no impurities. This was a significant improvement as the average reduction time prior to the addition of the iodine was 12.5 hours. This means that the regeneration stage is approximately 3.4 times faster with the addition of iodine which is able to activate the sodium by removing the passivation layer. Since re-testing the regeneration staged proved that sodium is better activated chemically with the addition of iodine, the control stage had to be re-tested to ensure that the Na^* would still be unable (or only slowly able) to reduce **2.6** (**Scheme 2.13E/Figure 2.12**).

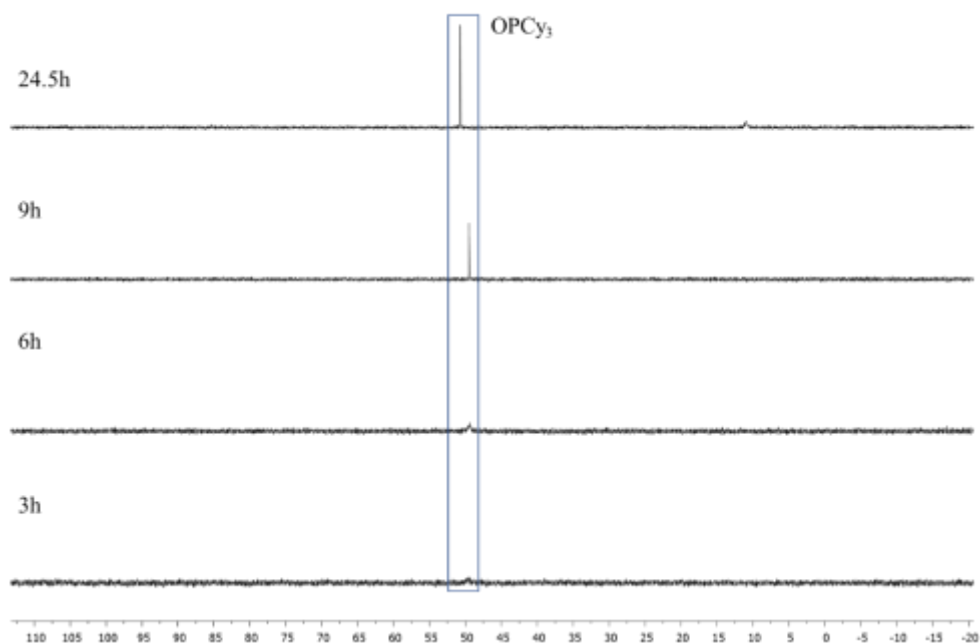
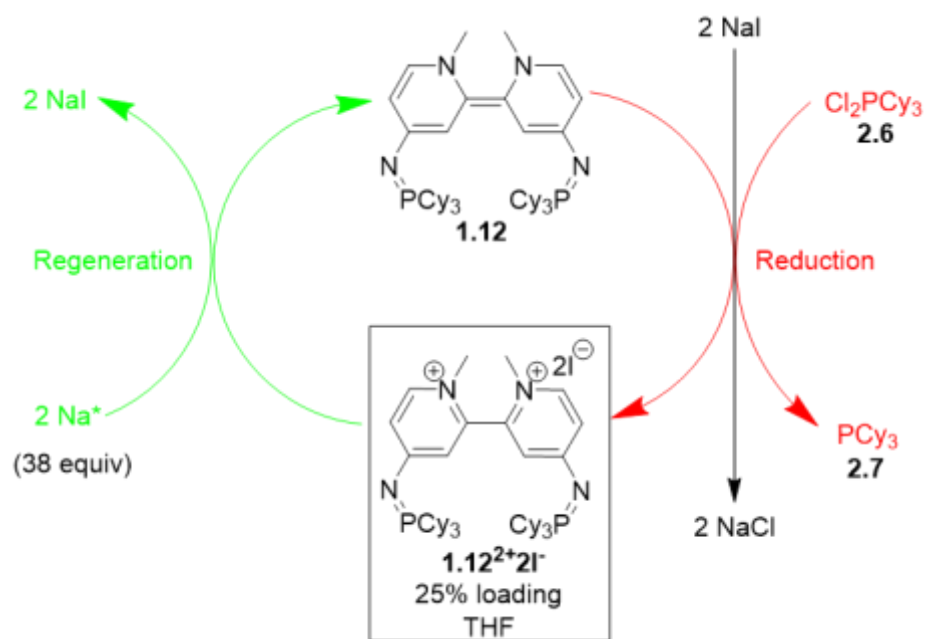


Figure 2.12: Stacked ^{31}P NMR spectra, monitoring the reduction of **2.6** via Na^* in THF over 24.5 hours.

Figure 2.12 shows the multiple stacked NMR spectra representative of one of three of the control tests monitored over 24.5h. As can be seen by the stacked spectra only trace amounts of **2.7** can be seen after 24.5h. It is important to note that much like the substrate **2.6** which has poor solubility in THF (**Figure 2.8**) the metathesized substrate (**2.11'**) also has poor solubility in THF which is why the peak representative of the substrate (approximately 106.3 ppm) is not visible in any of the above spectra. Some of the substrate was converted to tricyclohexylphosphine oxide (OPCy_3) which is represented by the peak at 49.5 ppm and is seen to grow over time. These results were promising as it proved that the Na^* was not very active in the conversion of Cl_2PCy_3 to PCy_3 . Following the re-testing of the control stage and regeneration stage the optimized catalytic cycle could be tested (**Scheme 2.14/Figure 2.13**).



Scheme 2.14: Catalytic cycle for the reduction of **2.6**.

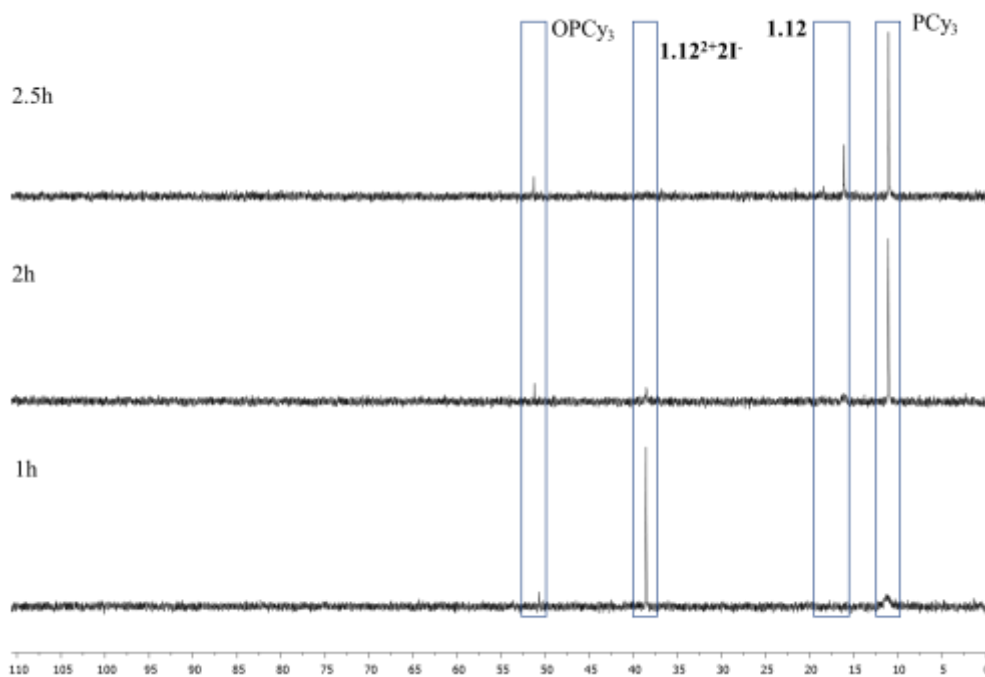


Figure 2.13: Stacked ³¹P NMR spectra, monitoring the reduction of **2.6** via the optimized catalytic cycle with 25% catalytic loading.

It can be seen above that using 25% catalyst loading, full reduction of **2.6** was achieved in 2.5 hours. This reaction time remained constant with two other trials. Based on ^{31}P NMR spectroscopy, approximately 91% of **2.6** was converted to **2.7** (11.0ppm) and 9% was converted to OPCy_3 (51.3ppm). The presence of BPY **1.12** (16.1ppm, 18.5ppm) is as expected since the large excess of sodium would convert all of $\mathbf{1.12}^{2+}2\mathbf{I}^-$ to **1.12** at the end of the reaction once all the substrate is consumed. Following the successful trials at 25% catalyst loading, the catalytic cycle was attempted again but with 12.5% and 5% catalyst loading (**Figure 2.14/2.15**).

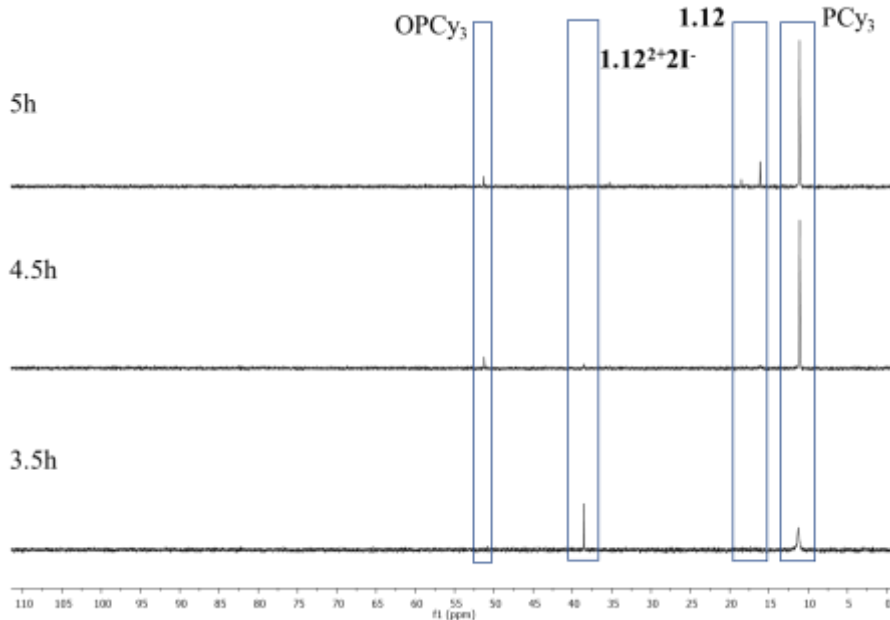


Figure 2.14: Stacked ^{31}P NMR spectra, monitoring the reduction of **2.6** via the optimized catalytic cycle with 12.5% catalyst loading.

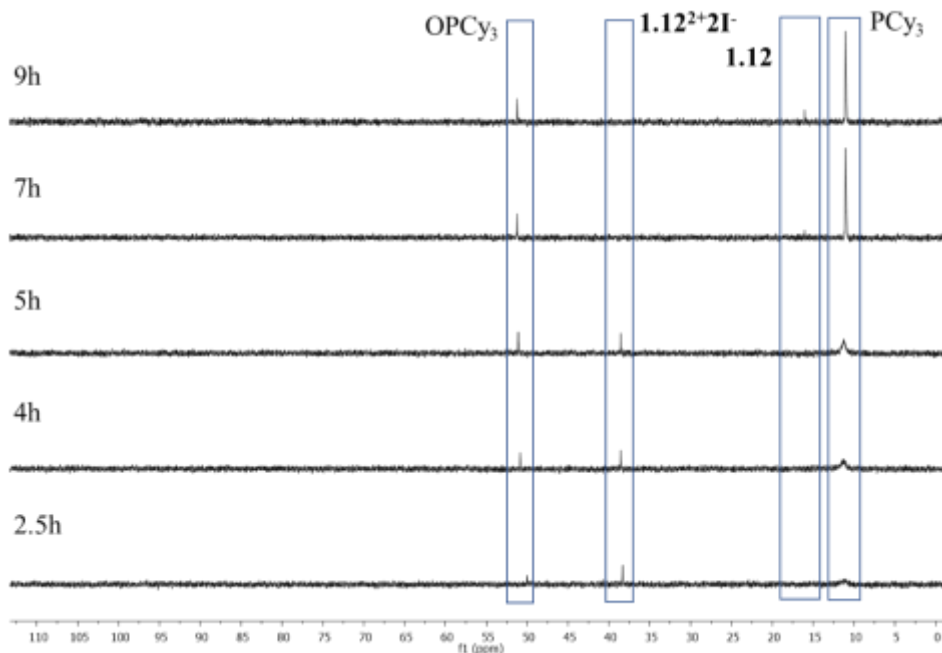
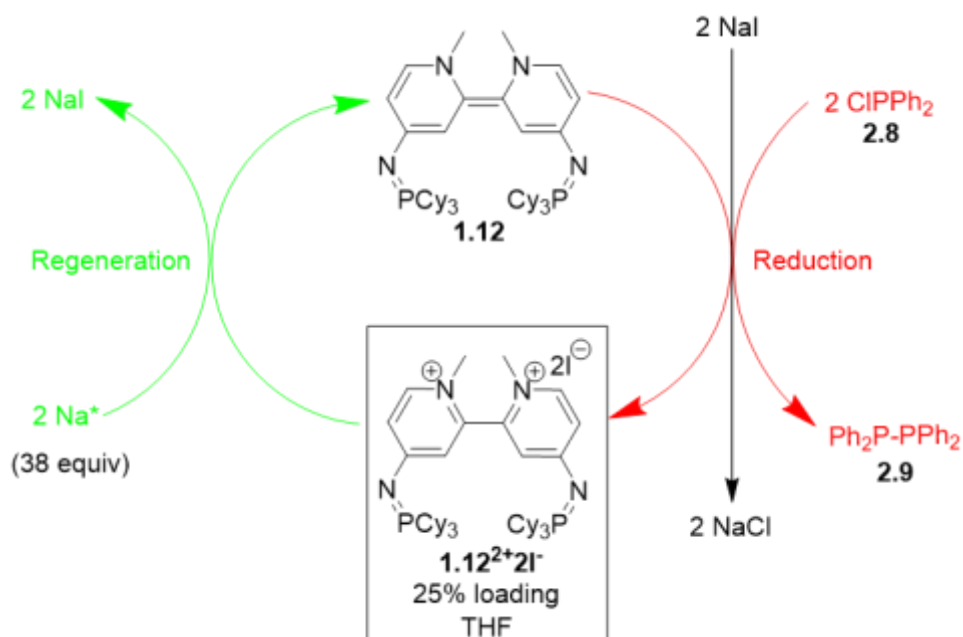


Figure 2.15: Stacked ^{31}P NMR spectra, monitoring the reduction of **2.6** via the optimized catalytic cycle with 5% catalyst loading.

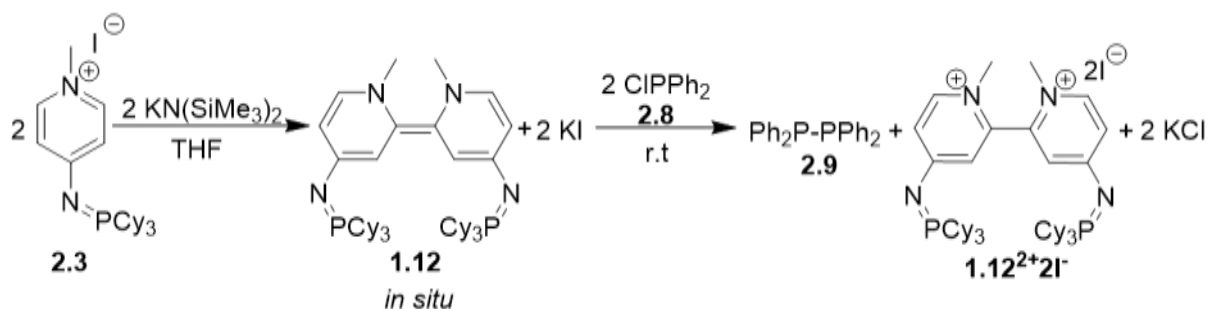
When using 12.5% catalyst loading (**Figure 2.14**), full reduction was achieved in 5 hours. At 3.5 hours both $\mathbf{1.12}^{2+2\Gamma}$ and **2.7** can be seen through ^{31}P NMR spectroscopy and after 5 hours the major peaks are representative of **2.7** and **1.12**. Approximately 3% of **2.6** was converted to OPCy_3 (50.1ppm). When using 5% catalyst loading (**Figure 2.15**) full reduction was achieved in approximately 9 hours. Oxidized BPY $\mathbf{1.12}^{2+2\Gamma}$ can be seen for the initial 5 hours of the reaction, as the peak representative of **2.7** progressively increases in intensity. In the final 4h of the reaction the intensity of **2.7** continues to increase suggesting that **2.6** is still being reduced, and at 9h **1.12** is visible, indicating that all of **2.6** has reacted. Approximately 90.1% of **2.6** was converted to **2.7** and the remaining 9.9% was converted to OPCy_3 . BPY **1.12** is only observed at the end of the reaction, with $\mathbf{1.12}^{2+2\Gamma}$ observed in the middle. This indicates that the conversion of oxidized BPY ($\mathbf{1.12}^{2+2\Gamma}$) to

BPY (**1.12**) is the rate limiting step and the BPY reacts rapidly with substrate, which agrees with the stoichiometric testing of the individual steps. Following the successful reduction of **2.6** at 5% catalytic loading, ClPPh₂ (**2.8**) was targeted as the next substrate to be reduced in the catalytic cycle (**Scheme 2.15**).



Scheme 2.15: Proposed catalytic cycle for the reduction of **2.8**.

Fortunately, as there is no change to the regeneration stage, only the reduction and control stage had to be tested for this new substrate before attempting the complete catalytic cycle. The first to be tested was the reduction stage (**Scheme 2.16**).



Scheme 2.16: Reduction of **2.8** through the use of **1.12** formed *in situ*.

It should also be noted that unlike **2.6**, substrate **2.8** is naturally a liquid, this means that it forms a homogenous mixture with **1.12/1.12²⁺2I⁻** even with the addition of the iodine (**Figure 2.16**).

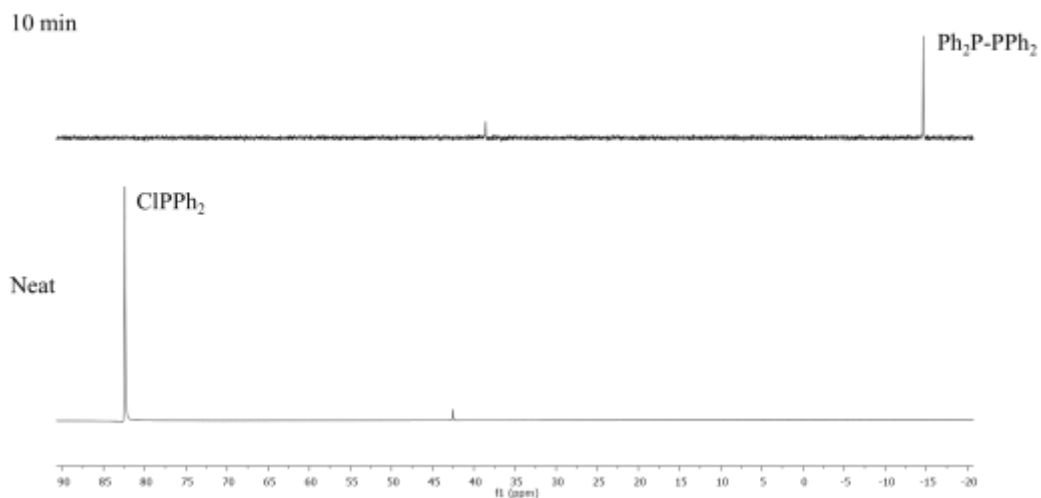


Figure 2.16: ^{31}P NMR spectrum of pure substrate **2.8** (bottom spectrum). ^{31}P NMR spectrum of the reaction mixture 10 minutes after the addition of **2.8** to BPY **1.12** (formed *in situ*, (top spectrum)).

Figure 2.16 shows that the neat substrate has a chemical shift of 82.4 ppm by ^{31}P NMR spectroscopy, which is consistent with the literature value (81.5 ppm).⁴² Substrate **2.8** is added to **1.12** (generated *in situ*) in THF. After 10 minutes it can be seen that full conversion occurred and $\mathbf{1.12}^{2+}2\mathbf{I}^{-}$ (38.6ppm) and **2.9** (-14.6ppm) can be seen by ^{31}P NMR spectroscopy. This agrees with the literature value for $\text{Ph}_2\text{P}-\text{PPh}_2$ (**2.9**) of -14.4ppm.⁵

Since **2.8** is naturally a liquid there was a chance that it would react with the highly active sodium much quicker than **2.6** (which is not completely soluble in THF in the presence of iodine). Due to this concern, it was important to monitor the control stage for substrate **2.8** closely (**Scheme 2.9**).



Scheme 2.17: Reduction of **2.8** through the use of Na.

The control stage showed that activated sodium was able to reduce **2.8** (**Figure 2.17**). Phosphine **2.8** (84.4ppm) was fully reduced after 10 minutes producing diphosphine **2.9** (-14.6ppm) and a trace amount of unknown impurity (-18.1 ppm). This means that the use of a BPY catalyst to reduce substrate **2.8** is not necessary since not only can the sacrificial donor (Na) reduce the substrate, but it can perform the reduction at a rate on par with BPY **1.12** at stoichiometric amounts.

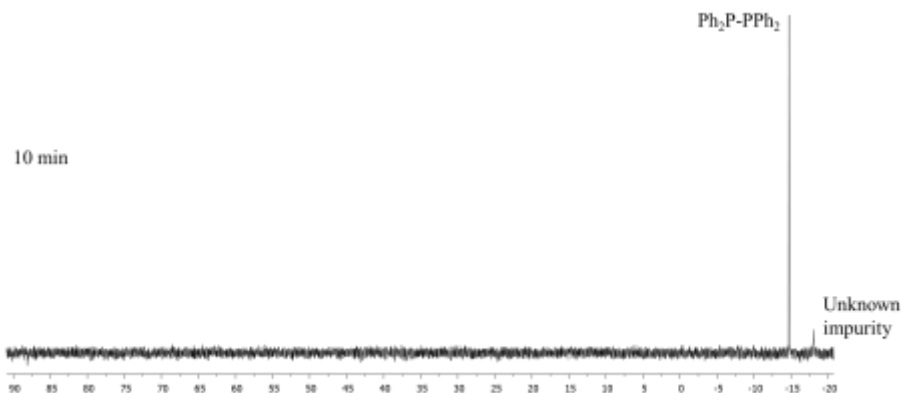
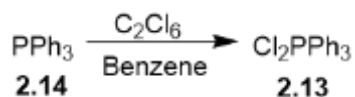


Figure 2.17: ^{31}P NMR spectrum of the reaction mixture 10 minutes after the addition of **2.8** to Na^* in THF.

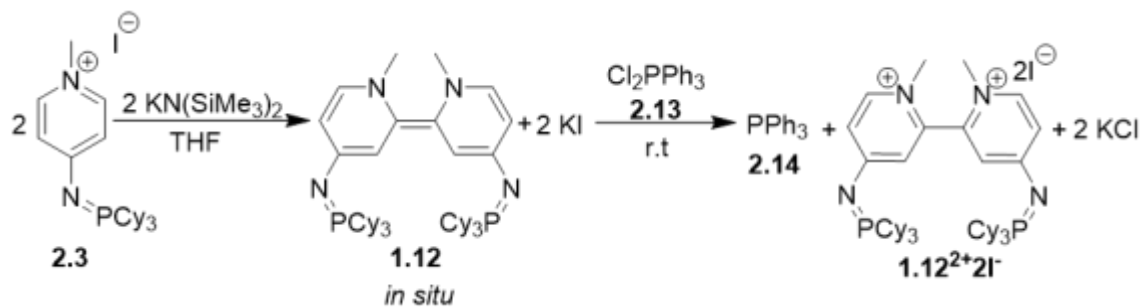
Moving forward, the next substrate that was selected to be tested for the catalytic cycle was dichlorotriphenylphosphorane (**2.13**). This substrate was prepared using an analogous procedure to that which was used to make **2.6** (**Scheme 2.18**).⁵



Scheme 2.18: Synthesis of dichlorotriphenylphosphorane (**2.13**).

It should be noted that dichlorotriphenylphosphorane was found to have a chemical shift of 62.0 ppm in acetonitrile (see appendix **Figure A7**), which corresponds well with the literature value (65.0 ppm).^{40,43} The chemical shift in THF is reported herein as -45.9 ppm. The large change in chemical shift due to solvent is because the pentavalent phosphine species is predominant in non-polar solvent (THF), and the ionic phosphine species is the predominant species in polar solvents (CH_3CN).^{41,43,44} It was thought that

testing this substrate would give better insight to the limitations of the developed catalytic cycle as it is structurally very similar to substrate **2.6**, however, it shows better solubility in THF. The reduction stage was the first to be tested (**Scheme 2.19**).



Scheme 2.19: Reduction of **2.13** via **1.12** (generated *in situ*).

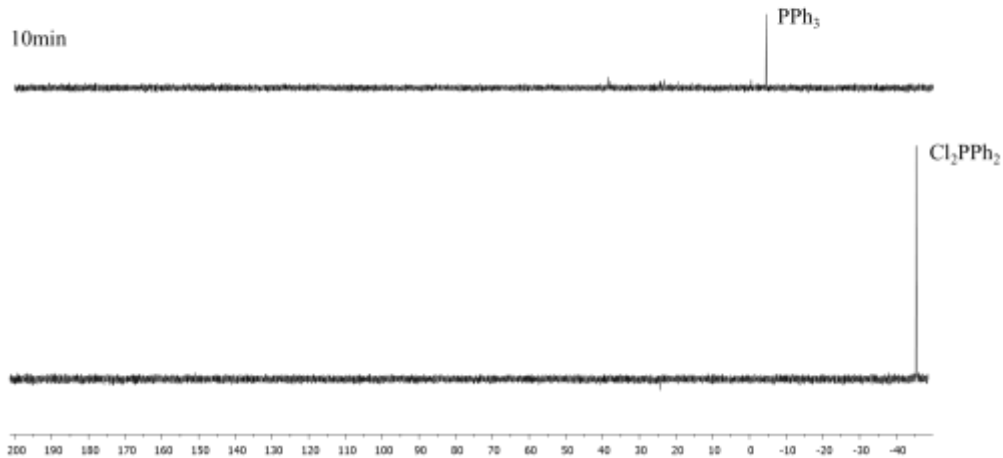


Figure 2.18: ^{31}P NMR spectrum of pure substrate **2.13** in THF (bottom spectrum). ^{31}P NMR spectrum of the reaction mixture 10 minutes after the addition of **2.13** to BPY **1.12** (formed *in situ*, (top spectrum)).

The reduction of **2.13** was carried out following the same procedure used for substrate **2.6** and **2.8** and produced similar results (**Figure 2.18**). The reduction of **2.10** was monitored through ^{31}P NMR spectroscopy. The bottom spectrum shows **2.13** prior to the addition of **1.12** (generated *in situ*). The reduction was complete 10 minutes after the addition of **1.12** to **2.13** (-45.5 ppm), and full conversion of **2.13** to **2.14** (-4.5 ppm) was observed. Oxidized BPY $\mathbf{1.12}^{2+}\mathbf{2I}^-$ cannot be seen, providing evidence that it most likely underwent a metathesis reaction to form $\mathbf{1.12}^{2+}\mathbf{2Cl}^-$. This is supported by the fact that precipitate was present in the reaction mixture. Much like the other two substrates, **2.13** was reduced quickly by BPY **1.12**. Following the positive results, the control test for **2.13** could be attempted (**Scheme 2.20**).



Scheme 2.20: Reduction of **2.13** via activated Na.

The control test for **2.13** would determine if it would be a viable substrate for the catalytic cycle. This control test also gave insight as to whether or not the catalytic cycle is useful for both substrates that form heterogenous and homogenous mixtures. **Figure 2.19** shows the results from the control test for substrate **2.13**.

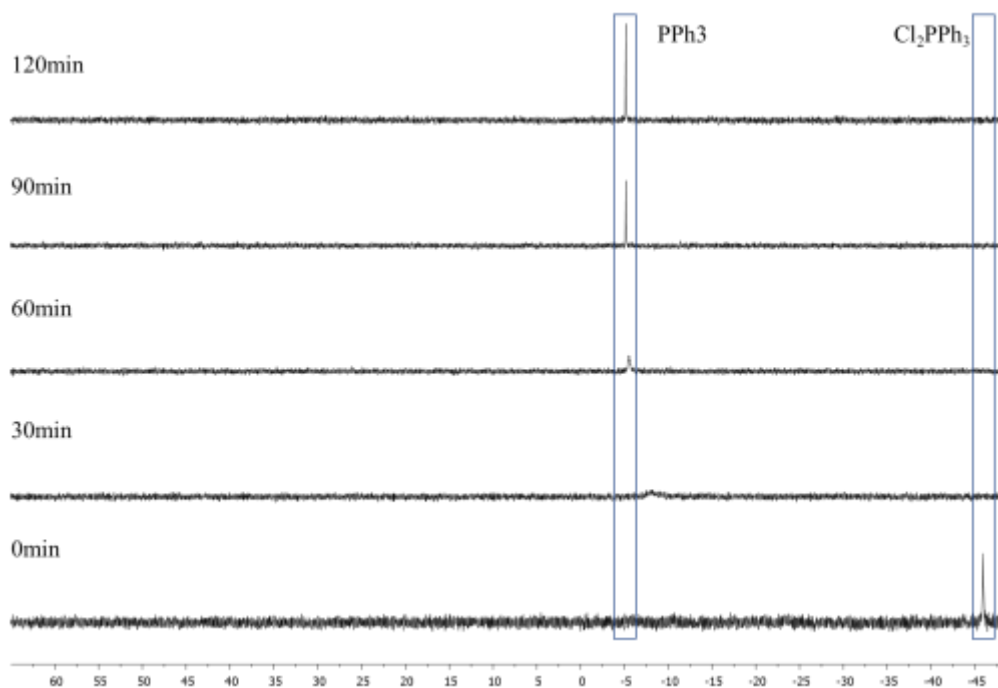


Figure 2.19: Stacked ^{31}P NMR spectra, monitoring the reduction of **2.13** via Na^* over 1.5h.

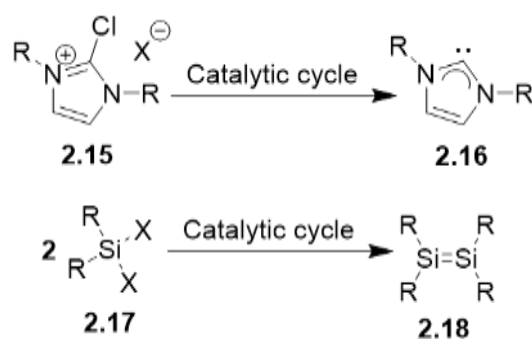
Full reduction of **2.13** was achieved via activated sodium in 2h. Phosphorane **2.13** (-45.9 ppm) was completely converted to **2.14** (-5.2 ppm) with no impurities. This means that the control test was unsuccessful as reduction occurred too quickly. The catalytic cycle would be unable to achieve a significant number of turnovers with BPY **1.12** in sub-stoichiometric amounts to fully reduce **2.13** in the time that it would take the activated sodium to reduce **2.13**. These results show that the catalytic methodology developed for Cy_3PCl_2 (**2.6**) is likely most viable for substrates that have poor solubility and remain undissolved in solution.

2.3: Conclusion and Future Work

In conclusion, a new catalytic cycle has been developed that uses a BPY derivative (**1.12**) as a catalyst. Through the application of this catalytic cycle, it was proven possible to successfully reduce dichlorotricyclohexylphosphorane (**2.6**) at 5% catalytic loading in 9h. Full reduction was achieved using minimal amounts of BPY, lowering the overall cost of the reduction. It was found that both chlorodiphenylphosphine (**2.8**), and dichlorotriphenylphosphorane (**2.13**), could easily be reduced using activated sodium at a reaction rate comparable to when **1.12** was used to perform the reduction. This means that the BPY catalyst is not required to achieve efficient reduction of the substrate. The results from compounds **2.8** and **2.13** also suggest that the catalytic cycle is most effective for substrates that remain insoluble in the reaction mixture such as substrate **2.6**. This is likely because both **2.8** and **2.13** are highly soluble and could easily undergo surface area reactions with the activated sodium.

Moving forward with this project there are numerous areas of study that should be explored. It is imperative that reduced phosphine **2.7** be isolated post catalysis and an accurate isolated yield should be determined. This needs to be done in order to prove that the reduced products produced through the catalytic cycle can be useful for subsequent reactions, similar to how they would be usable post reduction via a classical reducing agent (such as sodium). Should it also prove possible to isolate the BPY^{2+} post catalysis the limitations of its reusability could also be tested. The scalability of the catalytic cycle also needs to be investigated. A large-scale reduction of a substrate that is known to be reduced by the catalytic cycle (i.e., Cl_2PCy_3) needs to be performed to demonstrate that the catalytic cycle continues to be efficient on a larger, multigram scale. Different substrates should also

be continued to be tested to see if they are valid substrates to be reduced using the catalytic cycle. Other halogenated phosphines can be tested however, the substrate scope can be expanded beyond halogenated phosphines, so long as the reduction produces two stable non-basic anions. It may prove possible to reduce organohalogens such as imidazolium salts (**2.15**), in an effort to produce stable carbenes, and silicone-based compounds (**Scheme 2.21**). If the reduction of the imidazolium salt is successful via the catalytic cycle it would prove possible to form readily available carbenes that can be then used to form metal-carbene complexes that serve as efficient catalysts used widely in the pharmaceutical industry to develop various drugs, such as antimicrobial and anticancer agents.⁴⁵

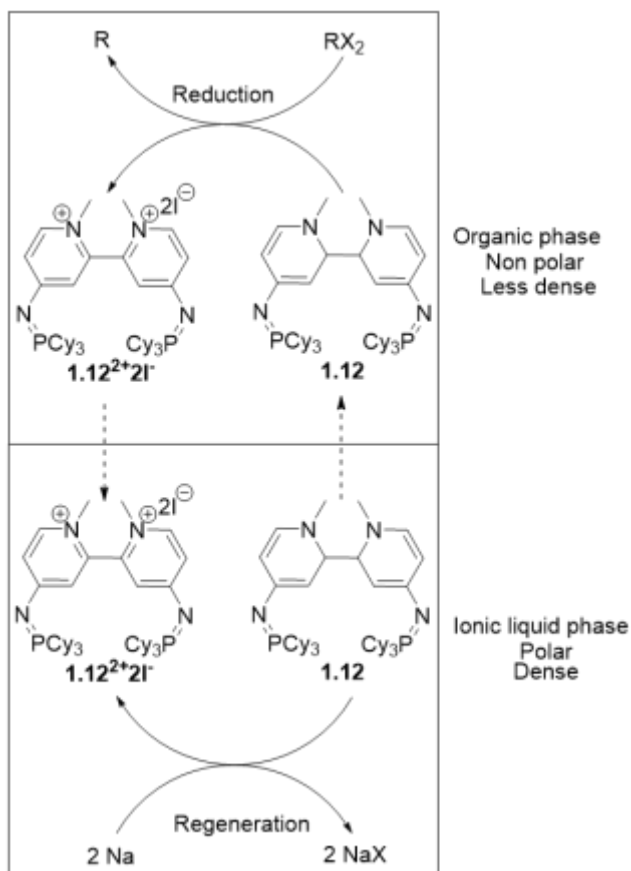


Scheme 2.21: General reduction of a carbene precursor and silane derivative through the use of 0.05 eq **1.12**, 40 eq Na*, THF.

Different sacrificial donors could be tested in an attempt to increase the rate of the regeneration stage. Since the regeneration of the BPY from BPY²⁺ is the rate limiting step, increasing the rate of that specific reaction should help to increase the rate of the overall catalytic cycle. This would potentially allow for an increase in the number of catalytic turnovers in a shorter period of time.⁴⁶ Chemical activation of previously tested sacrificial donors that were unable to reduce the oxidized BPY could also be attempted. It was

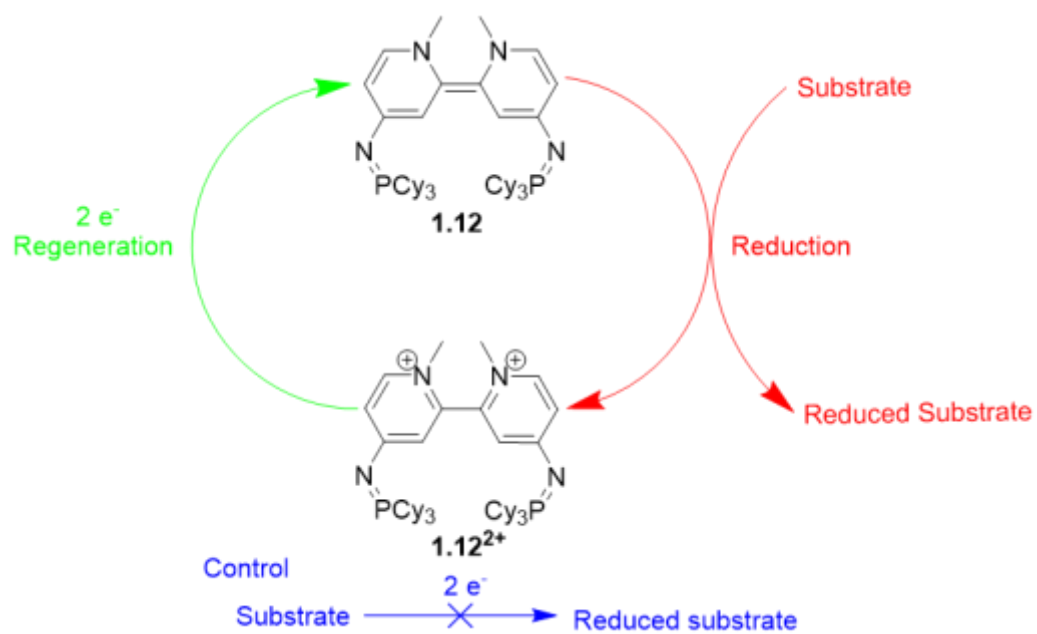
demonstrated herein that upon the activation of the sodium the regeneration of the BPY occurred 3.4x faster. It is possible that if lithium or magnesium were to be chemically activated that they would be able to reduce the oxidized BPY.

As opposed to using THF as a solvent it is possible that a two-phase solvent system would better facilitate the overall catalytic cycle. A biphasic system would consist of a non-polar (less dense) organic liquid, which would be optimal for the solubility of the BPY and many substrates such as various phosphines and silanes; and a second polar phase with higher density, such as an ionic liquid^{47,48} which will host the sodium (SD) and the oxidized BPY, optimizing its solubility, allowing it to be reduced to the BPY (**Scheme 2.22**). The density difference should allow for the organic phase to remain above the ionic liquid phase and for the compounds to exchange between phases. Using a biphasic solvent system could allow for the reduction of highly non-polar substrates via the catalytic cycle and could possibly overcome the limitations with regards to solubility of the substrate. It would also lead to a more general method since the sodium is separated from the substrate by the different phases however, the generation of a stable non-basic anion would still be a requirement of the substrate.



Scheme 2.22: Proposed biphasic catalytic cycle.

Finally, it may prove possible to develop an electrochemical catalytic cycle. As opposed to using a SD to regenerate the BPY from BPY^{2+} , this catalytic cycle would regenerate the BPY electrochemically (**Scheme 2.23**), removing the large amount of waste that is generated from the sacrificial donor. Similar to the catalytic cycle that was developed herein, all individual stages would need to be validated independently before the full catalytic cycle could be attempted.



Scheme 2.23: Proposed electrochemical catalytic cycle.

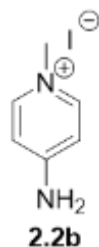
Chapter 3: Experimental

3.1: General Considerations

Unless otherwise stated, all experiments were performed under air and moisture free conditions and all reagents were obtained under the same conditions. Experiments were performed in an inert argon atmosphere through the use of an Innovative Technology glovebox or with standard Schlenk techniques. All solvents and reagents used were purchased through Sigma Aldrich or Oakwood Chemicals. Water and moisture free solvents were obtained from a Seca Solvent Dispensing System by Glass Contour, then degassed and stored over activated molecular sieves. Tetrahydrofuran (THF) required additional treatment to obtain the dryness required to perform certain reactions. THF was distilled from potassium/benzophenone, degassed, and stored over molecular sieves before being used. Nuclear Magnetic Resonance (NMR) spectroscopy was used as a means of primary analysis for each procedure. This was done using a Varian UNITY INOVA 300 MHz spectrometer and an internal reference of 85% phosphoric acid for all ^{31}P NMR spectra. Both the 300 MHz and an Agilent 400-MR NMR spectrometer were used to obtain ^1H spectra, in various deuterated solvents, with the spectrometers and solvents used for each procedure indicated in the corresponding procedures.

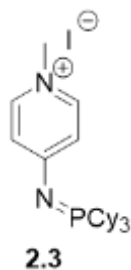
3.2: General Synthetic Procedures

Synthesis of pyridinium iodide **2.2b**



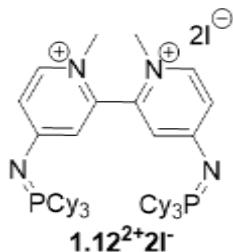
This procedure does not require air/moisture free conditions. Prepared following a known procedure.³³ 4-Aminopyridine (2.026 g, 21.53 mmol) was dissolved in acetone (48 mL). Iodomethane (1.6 mL, 25.73 mmol) was added dropwise over 5 minutes to the solution, while continuously stirring. After 30 minutes, diethyl ether (30 mL) was added to further promote precipitation. After stirring for an additional 5 minutes the white precipitate was collected by vacuum filtration and washed three times with diethyl ether (10 mL), and dried under vacuum, yielding **2.2b** (4.846 g, 97%). ¹H NMR (400 MHz, D₂O): δ 3.77 (s, 3H, CH₃), 6.70 (d, 2H, CH), 7.79 (d, 2H, CH).

Synthesis of 4-tricyclohexyliminophosphorano pyridine **2.3**



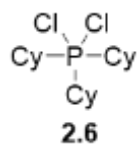
Prepared following a known procedure.³³ Tricyclohexylphosphine (1.180 g, 4.21 mmol) was dissolved in dichloromethane (13 mL). Hexachloroethane (1.062 g, 4.49 mmol) was added to the solution, and the mixture was stirred for 5 minutes. Triethylamine (1.5 mL, 10.76 mmol) was then added, resulting in an opaque mixture. **2.2b** (1.004 g, 3.58 mmol) was then added, and the reaction mixture was stirred for 2 hours. The reaction was removed from the inert atmosphere and distilled water (30 mL) was added to the solution. The organic phase was separated, dried over magnesium sulphate, and concentrated to near dryness under vacuum. Diethyl ether was then added to precipitate the product as a fine yellow powder which was subsequently filtered. The crude product was then recrystallized using isopropanol (30mL). The resulting fine yellow crystals were dried under vacuum (1.885 g, 86%). ³¹P NMR (300 MHz, CDCl₃): δ 5.7 (s, 1P,), **1H** NMR (300 MHz, CDCl₃): (**2.3**) δ 7.99 (d, 2H, CH), 6.71 (d, 2H, CH) 3.98 (s, 3H, CH₃), 1.17-2.37 (br, 33H, cyclohexane).

Synthesis of oxidized BPY $1.12^{2+}2I^-$



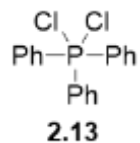
Prepared following modified known procedures.^{11,33} **2.3** (2.003 g, 3.89 mmol) was dissolved in toluene (25 mL). Potassium bis(trimethylsilyl)amide ((KHMDs) 0.961 g, 4.82 mmol) was added and the reaction mixture turned dark purple instantly. After 15 minutes the reaction mixture turned black. The reaction was stirred for 7 hours and the formation of **1.12** was confirmed using ^{31}P NMR spectroscopy. A solution of hexachloroethane (1.102 g, 4.65 mmol) dissolved in toluene (10 mL) was then added to the mixture over 2 minutes. No color change was observed and the reaction was stirred for 17 hours. The mixture was then removed from the inert atmosphere and hexanes (15 mL) was added which caused the formation of a brown precipitate. The reaction mixture was then filtered, and the precipitate was dissolved in chloroform (50 mL). H_2O (30 mL) was added to the solution and the organic phase was separated and dried over magnesium sulphate. The black filtrate was concentrated to near dryness under vacuum. Diethyl ether (20 mL) was added to cause the product to precipitate. The mixture was stirred vigorously for 12h then was subsequently filtered, and the light brown precipitate was then dried under vacuum, yielding a beige/brown solid (1.319g, 66%). ^{31}P NMR (300 MHz, CDCl_3): δ 38.4, (s, 2P **1.12 $^{2+}2I^-$**) ^1H NMR (300 MHz, CDCl_3): δ 8.14 (d, 2H, CH) 6.98 (d, 2H, CH) 6.75, (dd, 2H, CH), 3.83, (s, 6H, CH_3), 1.24-2.69, (m, 33H, cyclohexane).

Synthesis of dichlorotricyclohexylphosphorane (**2.6**)



Prepared following a known procedure.⁵ Tricyclohexylphosphine (2.004 g, 7.15 mmol) was dissolved in benzene (30 mL) before the slow addition of hexachloroethane (1.861 g, 7.86 mmol), resulting in a white precipitate. The reaction mixture was allowed to stir for 20 minutes before isolating the white solid via vacuum filtration. The product was washed with benzene (3 × 5mL) and dried under vacuum yielding **2.6** as a white powder (1.080 g, 43%). ³¹P NMR (300 MHz, THF): δ 97.8 (s, 1P, **2.6**).

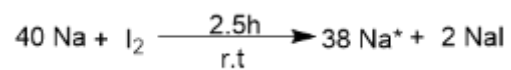
Synthesis of dichlorotriphenylphosphorane (**2.13**)



Triphenylphosphine (2.018 g, 7.69 mmol) was dissolved in benzene (30 mL) before the slow addition of hexachloroethane (1.843 g, 6.99 mmol). The solution was allowed to stir for 24h. A white precipitate had formed, and the solution remained clear. The solution was filtered, and the white precipitate was subsequently washed with hexanes (3x 10 ml) yielding **2.10** (1.151 g, 45%). ^{31}P NMR (300 MHz, THF): δ -45.2 (s, 1P, **2.10**).

3.3: Sodium activation

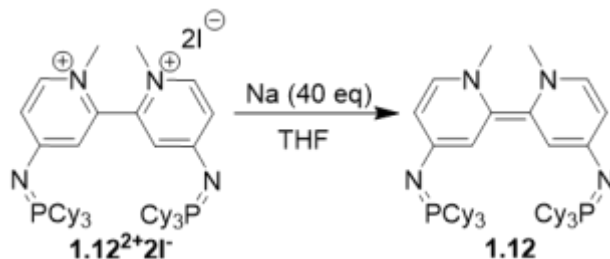
Sodium activation using iodine



Sodium (52.0 mg, 2.26 mmol) was cut into small pieces exposing a fresh surface and added to THF (4 mL). Iodine (14.4 mg, 0.06 mmol), a shiny grey solid, was then added to the reaction mixture, turning it dark red. The mixture was stirred for 2.5h until it became clear and colorless, and the remaining sodium was a shiny silver, indicating that all the iodine had reacted with the sodium.

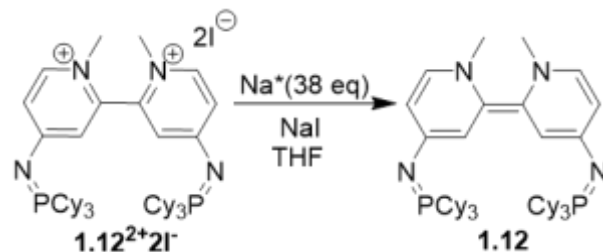
3.4: Regeneration Stage General Procedures

Reduction of $1.12^{2+}2I^-$ using sodium (Na)



Sodium (52.3 mg, 2.27 mmol) was cut into small pieces exposing a fresh surface and was stirred in THF (4 mL) for 1 hour. $1.12^{2+}2I^-$ (20.4 mg, 0.023 mmol) was then added to the THF/sodium mixture. The reaction immediately turned faint black. After approximately 1.5h the reaction mixture was notably darker, indicating the progression of the reaction. The reaction was monitored until completion, determined through ^{31}P NMR spectroscopy. ^{31}P NMR (300 MHz, CDCl₃): δ 18.6 (s, 2P (E isomer **1.12**)), 16.8 (s, 2P (Z isomer **1.12**)). Other characterization data was as reported.¹¹

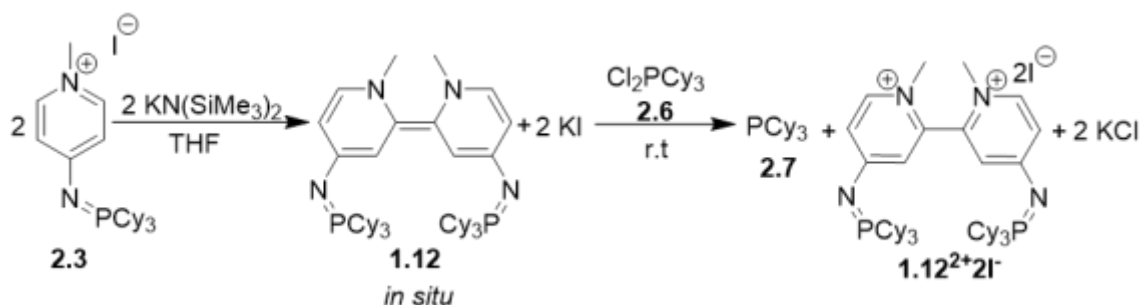
Reduction of $1.10^{2+}2I^-$ using activated sodium (Na^*)



Sodium (53.1 mg, 2.31 mmol) and iodine (14.2 mg, 0.056 mmol) were added to the reaction mixture as per the sodium activation procedure. Oxidized BPY **1.12**²⁺2I⁻ (19.8 mg, 0.0193 mmol) was then added to the THF/sodium mixture. The reaction immediately turned dark grey. After approximately 2h the reaction mixture was notably black/purple in color, indicating the progression of the reaction. The reaction was monitored until completion, determined through ³¹P NMR spectroscopy. ³¹P NMR (300 MHz, THF): δ 18.4 (s, 2P (E isomer **1.12**)), 16.0 (s, 2P (Z isomer **1.12**)).

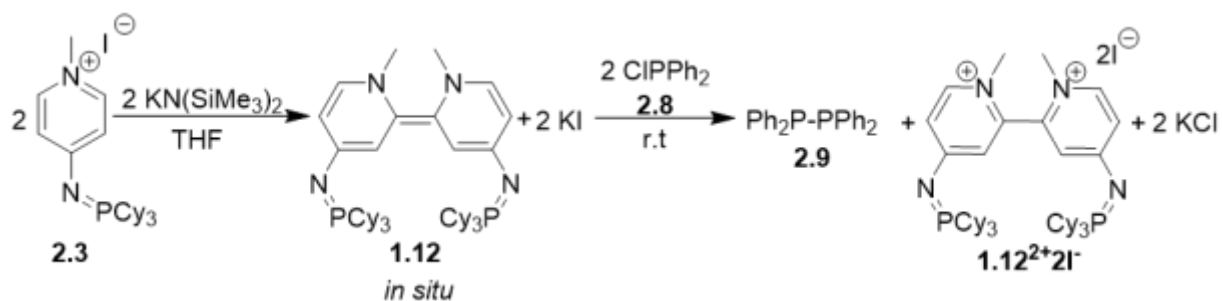
3.5: Reduction Stage General Procedures

Reduction of **2.6** via BPY **1.12** (*in situ*)



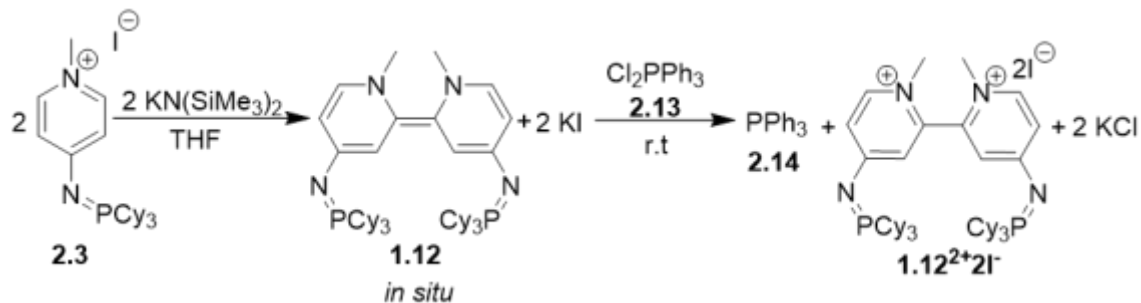
Pyridinium **2.3** (100.6 mg, 0.20 mmol) was dissolved in THF (4mL). KHMDS (42.7 mg, 0.21 mmol) was added, turning the solution dark purple immediately, which then turned dark black after 15 minutes. The reaction mixture was stirred for 7 hours to allow for the complete formation of BPY **1.12**. Full conversion of **2.3** to BPY **1.12** was confirmed through ^{31}P NMR spectroscopy. Substrate **2.6** (35.0 mg, 0.10 mmol) was added to the mixture over 2 minutes. After 10 minutes, the reaction turned light yellow with a light brown precipitate. BPY **1.12** and substrate **2.6** were absent in the reaction mixture, and both **2.7** and $\mathbf{1.12}^{2+}2\mathbf{I}^-$ were present as determined through ^{31}P NMR spectroscopy, indicating the reaction was complete. ^{31}P NMR (300 MHz, THF): δ 10.9 (s, 1P, PCy_3), 38.5 (s, 2P, $\mathbf{1.12}^{2+}2\mathbf{I}^-$) impurity: 45.6 (s, 1P, OPCy_3).

Reduction of **2.8** via BPY **1.12** (*in situ*)



Pyridinium **2.3** (40.6 mg, 0.04 mmol) was dissolved in THF (4 mL). KHMDS (16.0 mg, 0.08 mmol) was added, turning the solution dark purple immediately. The reaction mixture stirred for 7h to allow for the complete formation of BPY **1.12**. Full conversion of **2.3** to BPY **1.12** was confirmed through ^{31}P NMR spectroscopy. Substrate **2.8** (0.014 mL, 0.078 mmol) a clear colorless liquid, was added to the mixture. After 10 minutes the reaction was complete and **2.8** had converted to **2.9** and **1.12** had been converted to **1.12**²⁺**2I**⁻. This was confirmed through ^{31}P NMR spectroscopy. ^{31}P NMR (300 MHz, THF): δ -14.6 (s, 2P, **2.9**), 38.5 (s, 2P, **1.12**²⁺**2I**⁻).

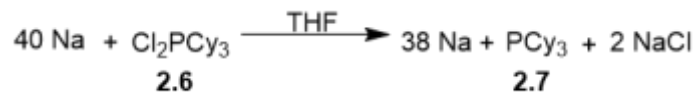
Reduction of **2.13** via BPY **1.12** (*in situ*)



Pyridinium **2.3** (124.0 mg, 0.24 mmol) was dissolved in THF (4 mL). KHMDS (48.0 mg, 0.24 mmol) was added, turning the solution dark purple immediately, which then turned dark black after 15 minutes. The reaction mixture stirred for 7 hours to allow for the complete formation of BPY **1.12**. Full conversion of **2.3** to BPY **1.12** was confirmed through ^{31}P NMR spectroscopy. Substrate **2.13** (40.3 mg, 0.12 mmol) was added to the mixture over 2 minutes. BPY **1.12** and substrate **2.10** were absent in the reaction mixture, and **2.14** was present as determined through ^{31}P NMR spectroscopy, indicating the reaction was complete. ^{31}P NMR (300 MHz, THF): δ -5.2 (s, 1P, PPh_3).

3.6: Control Stage General Procedures

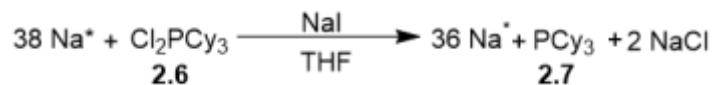
Reduction of **2.6** via sodium (Na)



Phosphorane **2.6** (20.1 mg, 0.06 mmol), a white solid, was added to THF (4 mL) and allowed to stir for 10 min. The solution remained clear and colorless and some of **2.6** remained undissolved as a white solid. Sodium (53.0 mg, 2.30 mmol) was cut into small pieces exposing fresh surface area and was added to the reaction mixture. The reaction was monitored through ^{31}P NMR spectroscopy. The solution turned cloudy and grey around 3h. The reaction was monitored for 3 days with no sign of reduction and only **2.6** was observed.

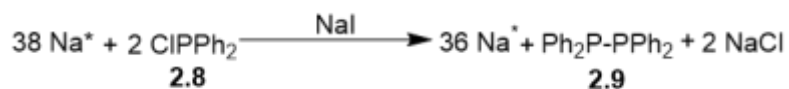
^{31}P NMR (300 MHz, THF): δ 97.8 (s, 1P, **2.6**).

Reduction of **2.6** via activated sodium (Na*)



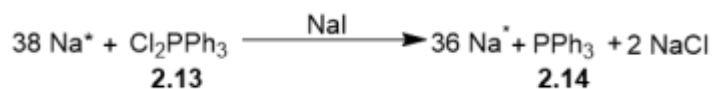
Sodium (52.0 mg, 2.26 mmol) and iodine (14.4 mg, 0.06 mmol) were added to the reaction mixture as per the sodium activation procedure. Phosphorane **2.6** (20.2 mg, 0.6 mmol) a white solid, was then added to the reaction mixture however remained undissolved as a solid in the reaction mixture. After monitoring the reaction for 24.5h it was determined through ³¹P NMR spectroscopy that there were only trace amounts of **2.7** present and a significant amount of **2.6** had been converted to phosphine oxide (OPCy₃). ³¹P NMR (300 MHz, THF): δ 10.9 (s, 1P, PCy₃), 49.5 (s, 1P, OPCy₃).

Reduction of **2.8** via activated sodium (Na*)



Sodium (84.0 mg, 3.65 mmol) and iodine (23.2 mg, 0.091 mmol) were added to the reaction mixture as per the sodium activation procedure. Substrate **2.8** (16.3 mg, 0.09 mmol) a clear colorless liquid, was then added to the reaction mixture. The solution turned light yellow immediately and remained that color for the duration of the reaction. The reaction was monitored through ^{31}P NMR spectroscopy. Full reduction was achieved in 10 minutes. Reduced substrate **2.9** and trace amounts of phosphine oxide (OPPh₂) were observed through ^{31}P NMR spectroscopy. ^{31}P NMR (300 MHz, THF): δ -14.6 (s, 2P, **2.9**), 40.1 (s, 1P OPPh₂).

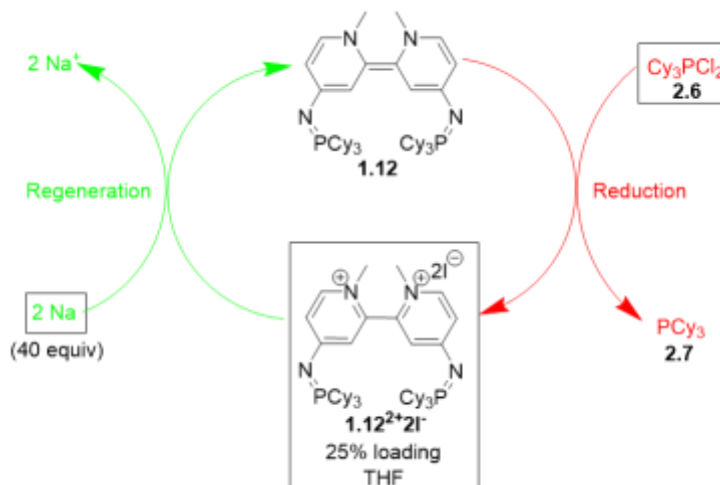
Reduction of **2.13** via activated sodium (Na*)



Sodium (55.7 mg, 2.42 mmol) and iodine (15.6 mg, 0.06 mmol) were added to the reaction mixture as per the sodium activation procedure. Phosphorane **2.13** (20.0 mg, 0.06 mmol), a light brown solid, was then added to the reaction mixture, the solution remained clear and colorless. After approximately 4h the solution began to turn dark red, the reaction was monitored through ^{31}P NMR spectroscopy. After 5h the reaction was complete, the solution remained dark red and the only compound visible through ^{31}P NMR spectroscopy was reduced substrate **2.14**. ^{31}P NMR (300 MHz, THF): δ -4.5 (s, 1P, PPh₃).

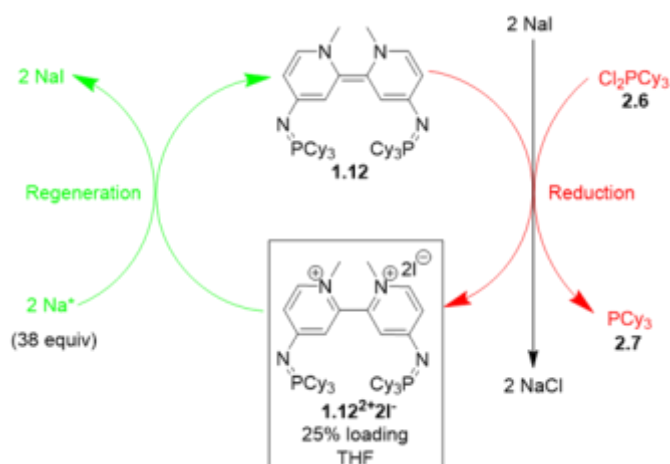
3.7: Catalytic Cycle General Procedures

Reduction of **2.6** via the complete catalytic cycle at 25% loading



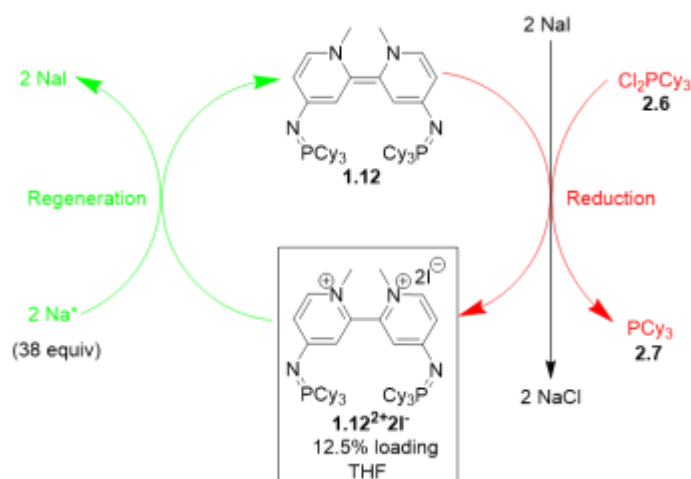
Phosphorane **2.6** (20.2 mg, 0.06 mmol) was dissolved in THF (4 mL). Oxidized BPY **1.12²⁺2I⁻** (12.3 mg, 0.01 mmol) was then added to the reaction mixture and remained undissolved. Sodium (53.3 mg, 2.32 mmol) was cut into small pieces exposing a fresh surface and was added to the reaction mixture. The reaction was monitored through ³¹P NMR spectroscopy over 3 days. After 3 days only **2.6** was visible through ³¹P NMR spectroscopy, indicating no reduction had occurred. ³¹P NMR (300 MHz, THF): δ 106.3 (s, 1P, PCy₃).

Reduction of 2.6 via the complete catalytic cycle at 25% loading using activated sodium (Na*)



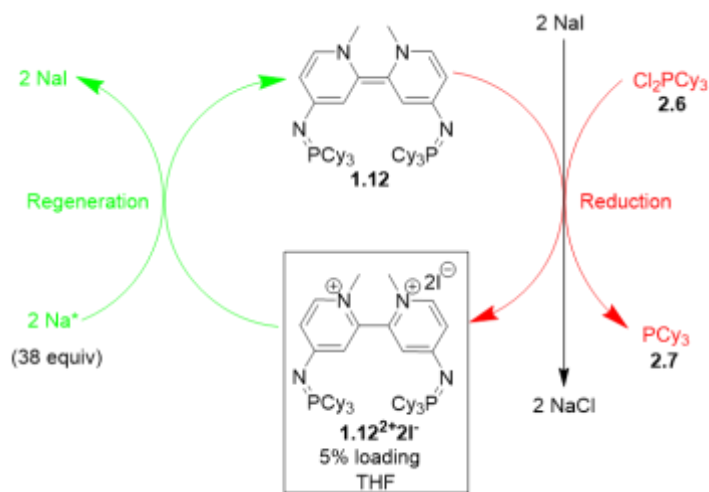
Sodium (52.7 mg, 2.29 mmol) and iodine (14.2 mg, 0.06 mmol) were added to the reaction mixture as per the sodium activation procedure. Oxidized BPY **1.12²⁺2I⁻** (14.5 mg, 0.01 mmol), a brown solid, was then added to the clear and colorless solution, turning the solution light brown. Phosphorane **2.6** (20.1 mg, 0.06 mmol), a white solid, was subsequently added and remained undissolved in the reaction mixture. The reaction was monitored through ³¹P NMR spectroscopy. Substrate **2.6** was fully reduced in 2.5h producing **2.7** and OPCy₃ as a minor impurity. BPY **1.12** remained in solution. ³¹P NMR (300 MHz, THF): δ 11.0 (s, 1P, PCy₃), 16.1 (s 2P (Z isomer **1.12**)), 18.5 (s 2P (E isomer **1.12**)), 51.3 (s 1P, OPCy₃).

Reduction of 2.6 via the complete catalytic cycle at 12.5% loading using activated sodium (Na*)



Sodium (52.7 mg, 2.29 mmol) and iodine (14.2 mg, 0.06 mmol) were added to the reaction mixture as per the sodium activation procedure. Oxidized BPY **1.12²⁺2I⁻** (14.5 mg, 0.01 mmol), a brown solid, was then added to the clear and colorless solution, turning the solution light brown. Phosphorane **2.6** (40.1 mg, 0.11 mmol), a white solid, was subsequently added and remained undissolved in the reaction mixture. The reaction was monitored through ^{31}P NMR spectroscopy. Substrate **2.6** was fully reduced in 5h producing **2.7** and OPCy_3 as a minor impurity. BPY **1.12** remained in solution. ^{31}P NMR (300 MHz, THF): δ 11.0 (s, 1P, PCy_3), 16.1 (s 2P (Z isomer **1.12**)), 18.5 (s 2P (E isomer **1.12**)), 51.3 (s 1P, OPCy_3).

Reduction of 2.6 via the complete catalytic cycle at 5% loading using activated sodium (Na*)



Sodium (53.1 mg, 2.30 mmol) and iodine (14.9 mg, 0.06 mmol) were added to the reaction mixture as per the sodium activation procedure. Oxidized BPY **1.12**²⁺**2I**⁻ (3.0 mg, 0.003 mmol), a brown solid, was then added to the clear and colorless solution, turning the solution light brown. Phosphorane **2.6** (20.7 mg, 0.06 mmol), a white solid, was subsequently added and remained undissolved in the reaction mixture. The reaction was monitored through ³¹P NMR spectroscopy. Substrate **2.6** was fully reduced in 2.5h producing **2.7** and OPCy₃ as a minor impurity. BPY **1.12** remained in solution. ³¹P NMR (300 MHz, THF): δ 11.0 (s, 1P, PCy₃), 16.1 (s 2P (Z isomer **1.12**)), 18.5 (s 2P (E isomer **1.12**)), 51.3 (s 1P, OPCy₃).

Bibliography

- (1) Broggi, J.; Terme, T.; Vanelle, P. *Angew. Chem Int. Ed.* **2014**, *53* (2), 384–413.
- (2) Schoenebeck, F.; Murphy, J. A.; Zhou, S. Z.; Uenoyama, Y.; Miclo, Y.; Tuttle, T. *J. Am. Chem. Soc.* **2007**, *129* (44), 13368–13369.
- (3) Murphy, J. A.; Gamier, J.; Park, S. R.; Schoenebeck, F.; Zhou, S. Z.; Turner, A. T. *Org. Lett.* **2008**, *10* (6), 1227–1230.
- (4) Doni, E.; Murphy, J. A. *Chem. Commun.* **2014**, *50* (46), 6073–6087.
- (5) Burgoyne, M. M.; Macdougall, T. M.; Haines, Z. N.; Conrad, J. W.; Calhoun, L. A.; Decken, A.; Dyker, C. A. *Org. Biomol. Chem.* **2019**, *17* (45), 9726–9733.
- (6) O’Sullivan, S.; Doni, E.; Tuttle, T.; Murphy, J. A. *Angew. Chem Int. Ed.* **2014**, *53* (2), 474–478.
- (7) Cutulic, S. P. Y.; Findlay, N. J.; Zhou, S. Z.; Chrystal, E. J. T.; Murphy, J. A. *J. Org. Chem.* **2009**, *74* (22), 8713–8718.
- (8) Cutulic, S. P. Y.; Murphy, J. A.; Farwaha, H.; Zhou, S. Z.; Chrystal, E. *Synlett* **2008**, No. 14, 2132–2136.
- (9) Zhou, S.; Farwaha, H.; Murphy, J. A. *Chimia (Aarau)*. **2012**, *66* (6), 418–424.
- (10) Murphy, J. A. *J. Org. Chem.* **2014**, *79* (9), 3731–3746.
- (11) Hanson, S. S. University of New Brunswick, 2010.
- (12) Lei, P.; Ding, Y.; Zhang, X.; Adijiang, A.; Li, H.; Ling, Y.; An, J. *Org. Lett.* **2018**, *20* (12), 3439–3442.
- (13) Markowitz, M. M. *J. Chem. Educ* **1963**, *40* (12), 633–636.
- (14) Monagheddu, M.; Doppiu, S.; Cocco, G. *J. Mater. Synth. Process.* **2000**, *8* (5–6), 295–300.

- (15) Hanson, S. S.; Richard, N. A.; Dyker, C. A. *Chem. Eur. J.* **2015**, *21* (22), 8052–8055.
- (16) Cox, N.; Dang, H.; Whittaker, A. M.; Lalic, G. *Tetrahedron* **2014**, *70* (27–28), 4219–4231.
- (17) Jolly, P. I.; Fleary-Roberts, N.; O’Sullivan, S.; Doni, E.; Zhou, S.; Murphy, J. A. *Org. Biomol. Chem.* **2012**, *10* (30), 5807–5810.
- (18) Cyran, M. K. *Chem. Rev.* **2005**, *105* (10), 3773–3811.
- (19) Zhang, D.; Telo, J. P.; Liao, C.; Hightower, S. E.; Clennan, E. L. *J. Phys. Chem. A* **2007**, *111* (51), 13567–13574.
- (20) Burkholder, C.; Dolbier, W. R.; Médebielle, M. *J. Org. Chem.* **1998**, *63* (16), 5385–5394.
- (21) Pop, F.; Amacher, A.; Avarvari, N.; Ding, J.; Daku, L. M. L.; Hauser, A.; Koch, M.; Hauser, J.; Liu, S. X.; Decurtins, S. *Chem. Eur. J.* **2013**, *19* (7), 2504–2514.
- (22) Zhang, D.; Dufek, E. J.; Clennan, E. L. *J. Org. Chem.* **2006**, *71* (1), 315–319.
- (23) Richard, N. A.; Khor, C. K.; Hetherington, S. M.; Mills, S. L.; Decken, A.; Dyker, C. A. *Chem. Eur. J.* **2020**, *26* (72), 17371–17375.
- (24) Tolman, C. A. *Chem. Rev.* **1977**, *77* (3), 313–348.
- (25) Hanson, S. S.; Doni, E.; Traboulsee, K. T.; Coulthard, G.; Murphy, J. A.; Dyker, C. A. *Angew. Chem Int. Ed.* **2015**, *54* (38), 11236–11239.
- (26) Frenette, B. L.; Arsenault, N.; Walker, S. L.; Decken, A.; Dyker, C. A. *Chem. Eur. J.* **2021**, *27* (33), 8528–8536.
- (27) Rohrbach, S.; Shah, R. S.; Tuttle, T.; Murphy, J. A. *Angew. Chem Int. Ed.* **2019**, *58* (33), 11454–11458.

- (28) Roberts, B. P. *Chem. Soc. Rev.* **1999**, 28 (1), 25–35.
- (29) Pan, X.; Lacôte, E.; Lalevée, J.; Curran, D. P. *J. Am. Chem. Soc.* **2012**, 134 (12), 5669–5674.
- (30) Li, N.; Pan, X. *Chinese J. Polym. Sci* **2021**, 39 (9), 1084–1092.
- (31) Garnier, J.; Murphy, J. A.; Zhou, S. Z.; Turner, A. T. *Synlett* **2008**, No. 14, 2127–2131.
- (32) Caramella, P.; Houk, K. . *Tetrahedron Lett.* **1981**, 22 (9), 819–822.
- (33) Frenette, B.; Aresenault, N.; Walker, S.; Decken, A.; Dyker, C. A. WILEY-VCH 2015, pp 11236–11239.
- (34) De, S.; Ghosh, S.; Bhunia, S.; Sheikh, J. A.; Bisai, A. *Org. Lett.* **2012**, 14 (17), 4466–4469.
- (35) Krawietz, T. R.; Murray, D. K.; Haw, J. F. *J. Phys. Chem. A* **1998**, 102 (45), 8779–8785.
- (36) Maryasin, B.; Zipse, H. *Phys. Chem. Chem. Phys* **2011**, 13, 5150–5158.
- (37) Goldwhite, H.; Kaminski, J.; Millhauser, G.; Ortiz, J.; Vargas, M.; Vertal, L.; Lappert, M. F.; Smith, S. J. *J. Organomet. Chem.* **1986**, 310 (1), 21–25.
- (38) Panda, T. K.; Kaneko, H.; Pal, K.; Tsurugi, H.; Mashima, K. *Organometallics* **2010**, 29 (11), 2610–2615.
- (39) Dilworth, J. R.; Hussain, W.; Hutson, A. J.; Jones, C. J.; Mcquillan, F. S.; Mayer, J. M.; Arterburn, J. B. *Inorg. Synth.* **2007**, 31, 257–262.
- (40) Gonnella, N. C.; Busacca, C.; Campbell, S.; Eriksson, M.; Grinberg, N.; Bartholomeyzik, T.; Shengli, M.; Norwood, D. L. *Magn. Reson. Chem.* **2009**, 47 (6), 461–464.

- (41) Dillon, K. B.; Lincoln, J. *The Structures Of Ph₃PICl And Ph₃PIBr*; Polyhedron, 1989; Vol. 8, 1445-1446
- (42) Moedritzer, K.; Maier, L.; Leo, G. *J. Chem. Eng. Data* **1962**, 7, 307–310.
- (43) Wiley, G. A. *Tetrahedron* **1967**, No. 24, 2321–2324.
- (44) Dillion, K.; Waddington, T. *Nat. Chem.* **1971**, 230, 159.
- (45) Koch, G. *Futur. Med Chem* **2015**, 71 (10), 1305–1333.
- (46) Engel, T.; Reid, P. *Thermodynamics, Statistical Thermodynamics, and Kinetics*, 4th ed.; Pearson, 2006.
- (47) Magna, L.; Morvan, D. *Appl. Catal. A. Gen* **2010**, 373, 1–56.
- (48) Wasserscheid, P.; Keim, W. *Angew. Chem Int. Ed.* **2000**, 39, 3772–3789.

Appendix

Selected NMR Spectra²⁸

In order of appearance from the experimental procedures in **Chapter 3**.

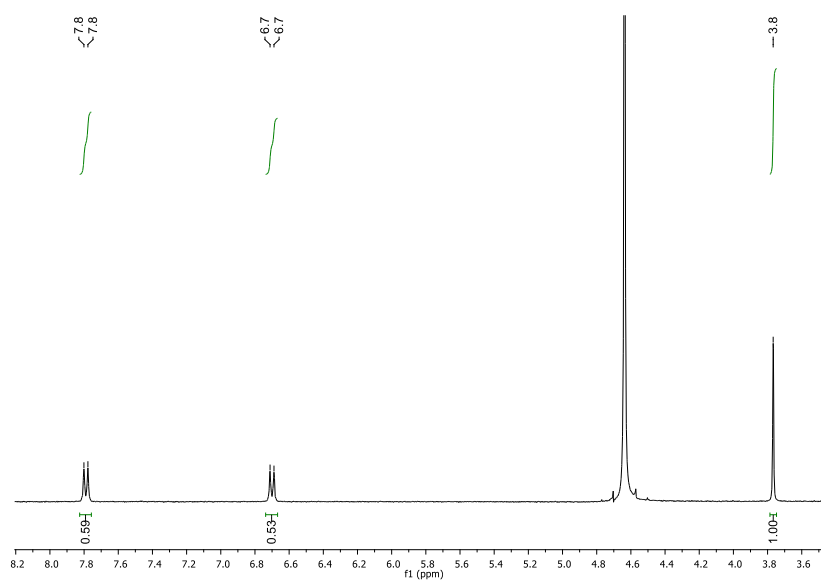


Figure A1: ¹H NMR spectra of 1-methyl-4-aminopyridine in D₂O.

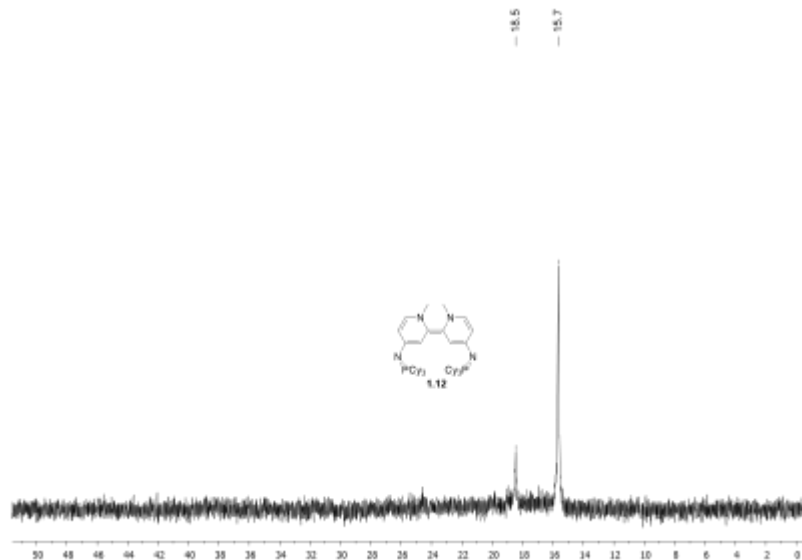


Figure A2: ^{31}P NMR spectra of BPY **1.12** (*in situ*) formation from **2.3** in toluene.

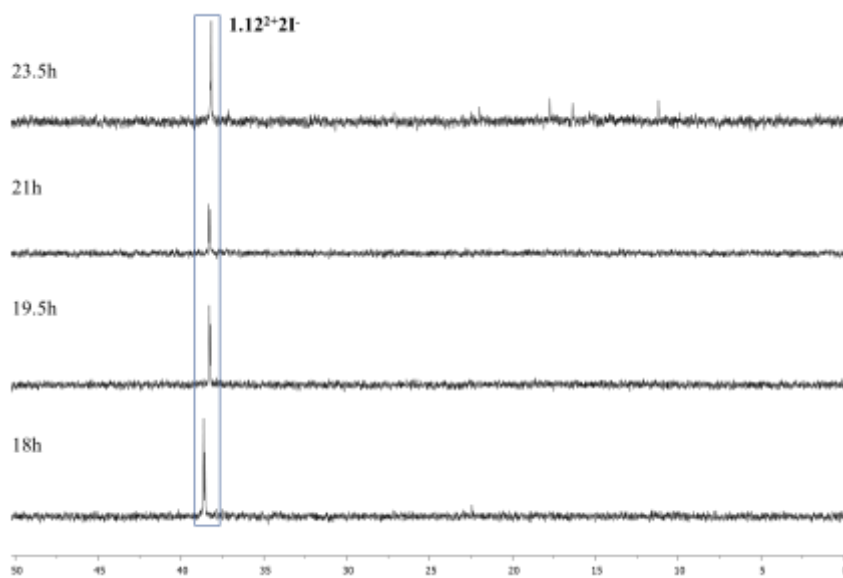


Figure A3: Stacked ^{31}P NMR spectra, monitoring the reduction of **1.12** $^{2+}$ with Li in THF over 23.5 hours.

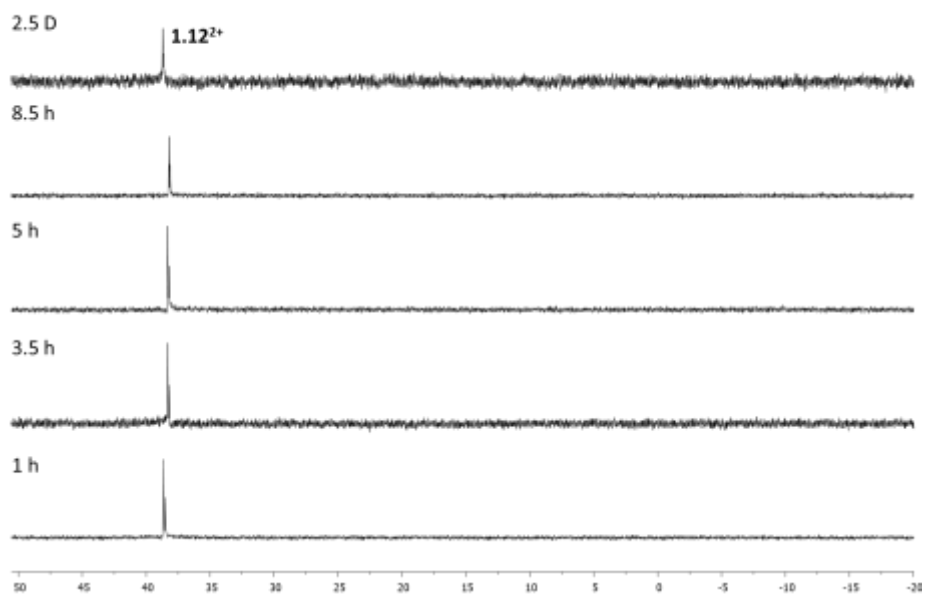


Figure A4: Stacked ^{31}P NMR spectra, monitoring the reduction of 1.12^{2+} with Mg in THF over 2.5 days.

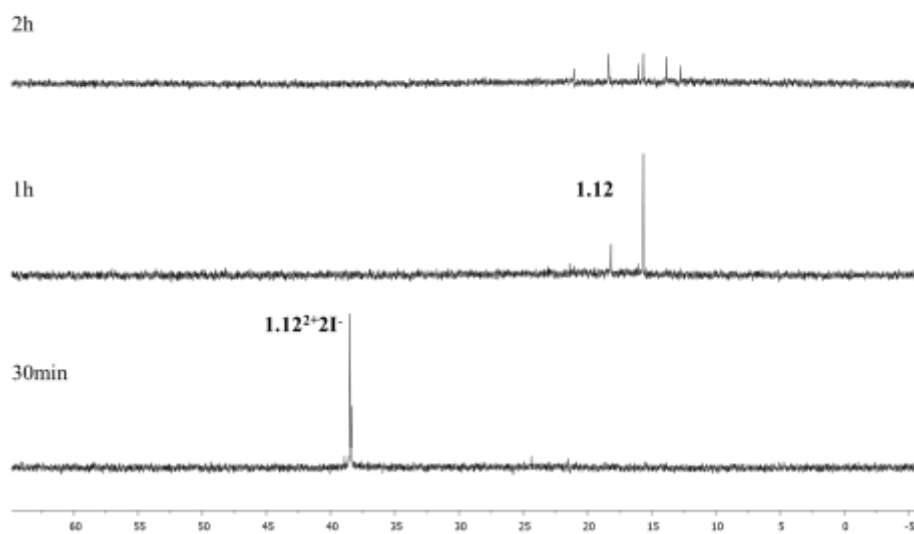


Figure A5: Stacked ^{31}P NMR spectra, monitoring the reduction of $1.12^{2+}2\text{I}^-$ with K in THF over 2h hours.

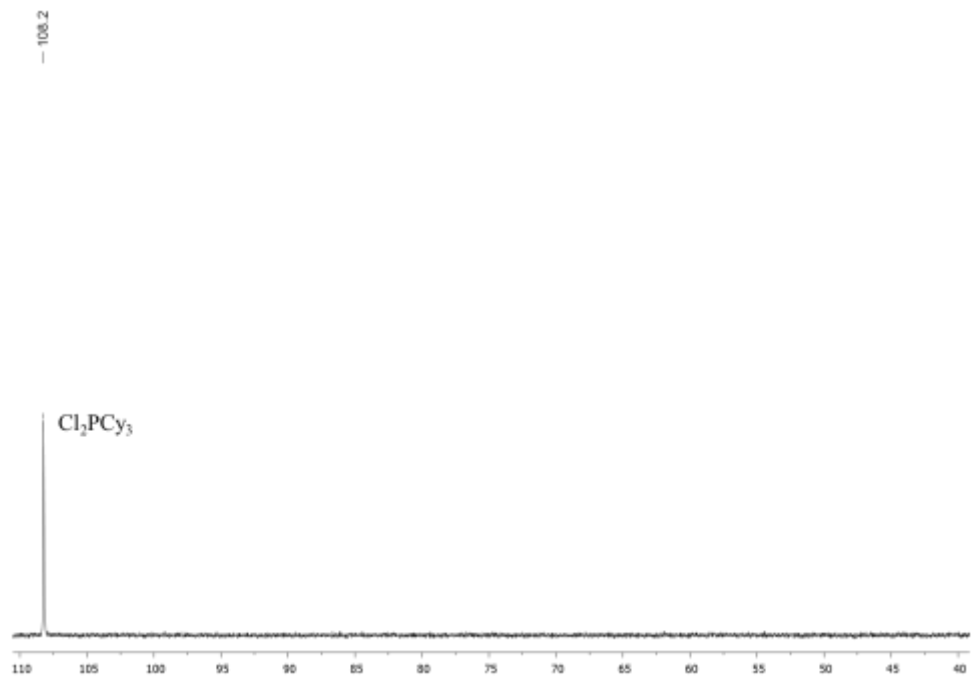


Figure A6: ^{31}P NMR spectrum of **2.6** and 1eq. of iodine.

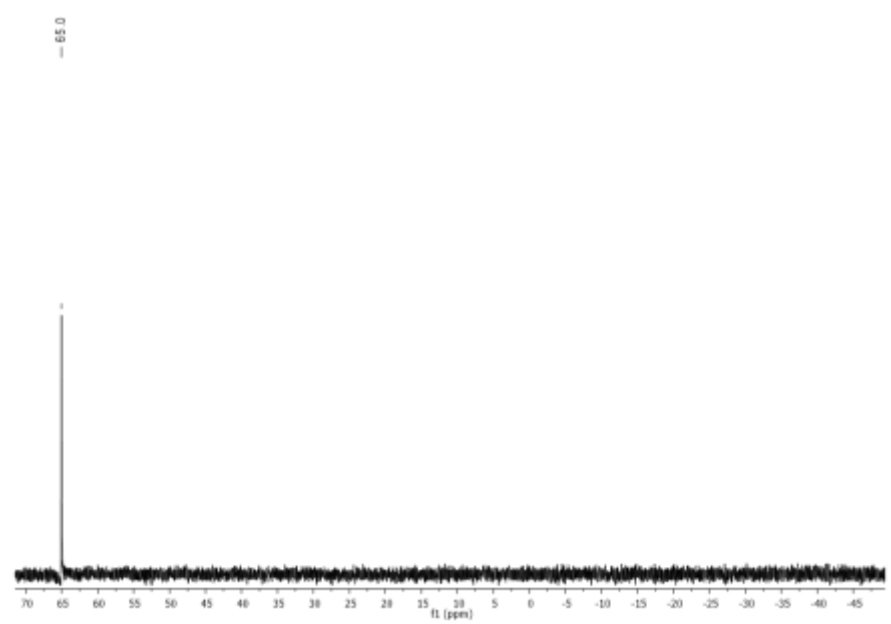


Figure A7: ^{31}P NMR of dichlorotriphenylphosphorane (**2.13**) in acetonitrile.

Curriculum Vitae

Candidate's full name: Zachary Lucas Rees

Universities Attended:

University of New Brunswick, Fredericton, NB Canada (Bachelor of Science Honors, Medicinal Chemistry, **2016-2020**)

Thesis: Turning Organic Reducing Agents Catalytic (Supervisor: Dr. C. Adam Dyker)

University of New Brunswick, Fredericton, NB Canada (Master of Science, Inorganic Chemistry, **2020-2021**)

Thesis: Turning Organic Reducing Agents Catalytic (Supervisor: Dr. C. Adam Dyker)

Publications: None

Conference Presentations: None